

Measurement of the Higgs boson mass with $H \rightarrow \gamma\gamma$ decays in 140 fb^{-1} of $\sqrt{s}=13 \text{ TeV}$ pp collisions with the ATLAS detector

ATLAS Collaboration

DOI:

[10.1016/j.physletb.2023.138315](https://doi.org/10.1016/j.physletb.2023.138315)

License:

Creative Commons: Attribution (CC BY)

Document Version

Version created as part of publication process; publisher's layout; not normally made publicly available

Citation for published version (Harvard):

ATLAS Collaboration 2023, 'Measurement of the Higgs boson mass with $H \rightarrow \gamma\gamma$ decays in 140 fb^{-1} of $\sqrt{s}=13 \text{ TeV}$ pp collisions with the ATLAS detector', *Physics Letters B*. <https://doi.org/10.1016/j.physletb.2023.138315>

[Link to publication on Research at Birmingham portal](#)

General rights

Unless a licence is specified above, all rights (including copyright and moral rights) in this document are retained by the authors and/or the copyright holders. The express permission of the copyright holder must be obtained for any use of this material other than for purposes permitted by law.

- Users may freely distribute the URL that is used to identify this publication.
- Users may download and/or print one copy of the publication from the University of Birmingham research portal for the purpose of private study or non-commercial research.
- User may use extracts from the document in line with the concept of 'fair dealing' under the Copyright, Designs and Patents Act 1988 (?)
- Users may not further distribute the material nor use it for the purposes of commercial gain.

Where a licence is displayed above, please note the terms and conditions of the licence govern your use of this document.

When citing, please reference the published version.

Take down policy

While the University of Birmingham exercises care and attention in making items available there are rare occasions when an item has been uploaded in error or has been deemed to be commercially or otherwise sensitive.

If you believe that this is the case for this document, please contact UBIRA@lists.bham.ac.uk providing details and we will remove access to the work immediately and investigate.

Journal Pre-proof

Measurement of the Higgs boson mass with $H \rightarrow \gamma\gamma$ decays in 140 fb^{-1} of $\sqrt{s} = 13 \text{ TeV}$ pp collisions with the ATLAS detector

The ATLAS Collaboration

PII: S0370-2693(23)00649-4
DOI: <https://doi.org/10.1016/j.physletb.2023.138315>
Reference: PLB 138315

To appear in: *Physics Letters B*

Received date: 16 August 2023
Revised date: 18 October 2023
Accepted date: 3 November 2023



Please cite this article as: The ATLAS Collaboration, Measurement of the Higgs boson mass with $H \rightarrow \gamma\gamma$ decays in 140 fb^{-1} of $\sqrt{s} = 13 \text{ TeV}$ pp collisions with the ATLAS detector, *Physics Letters B*, 138315, doi: <https://doi.org/10.1016/j.physletb.2023.138315>.

This is a PDF file of an article that has undergone enhancements after acceptance, such as the addition of a cover page and metadata, and formatting for readability, but it is not yet the definitive version of record. This version will undergo additional copyediting, typesetting and review before it is published in its final form, but we are providing this version to give early visibility of the article. Please note that, during the production process, errors may be discovered which could affect the content, and all legal disclaimers that apply to the journal pertain.

© 2023 Published by Elsevier.

EUROPEAN ORGANISATION FOR NUCLEAR RESEARCH (CERN)



Submitted to: Phys. Lett. B.

CERN-EP-2023-160
6th November 2023

Measurement of the Higgs boson mass with $H \rightarrow \gamma\gamma$ decays in 140 fb^{-1} of $\sqrt{s} = 13 \text{ TeV}$ pp collisions with the ATLAS detector

The ATLAS Collaboration

The mass of the Higgs boson is measured in the $H \rightarrow \gamma\gamma$ decay channel, exploiting the high resolution of the invariant mass of photon pairs reconstructed from the decays of Higgs bosons produced in proton–proton collisions at a centre-of-mass energy $\sqrt{s} = 13 \text{ TeV}$. The dataset was collected between 2015 and 2018 by the ATLAS detector at the Large Hadron Collider, and corresponds to an integrated luminosity of 140 fb^{-1} . The measured value of the Higgs boson mass is $125.17 \pm 0.11 \text{ (stat.)} \pm 0.09 \text{ (syst.) GeV}$ and is based on an improved energy scale calibration for photons, whose impact on the measurement is about four times smaller than in the previous publication. A combination with the corresponding measurement using 7 and 8 TeV pp collision ATLAS data results in a Higgs boson mass measurement of $125.22 \pm 0.11 \text{ (stat.)} \pm 0.09 \text{ (syst.) GeV}$. With an uncertainty of 1.1 per mille, this is currently the most precise measurement of the mass of the Higgs boson from a single decay channel.

Contents

1	Introduction	2
2	The ATLAS detector	3
3	Data and simulation samples	4
	3.1 Data	4
	3.2 Simulation samples	4
4	Event selection and classification	5
5	Mass measurement procedure	8
6	Systematic uncertainties	10
7	Results	12
8	Conclusion	16

1 Introduction

After the ATLAS and CMS collaborations at the Large Hadron Collider (LHC) discovered in 2012 [1, 2] a particle H with properties consistent with those of the Higgs boson in the Standard Model (SM) of particle physics, the precise determination of its mass became one of the primary goals of their physics programmes. The Higgs boson mass m_H is a fundamental parameter of the SM and the only unknown parameter of the scalar sector of the Standard Model prior to the Higgs boson discovery. Its measurement is of paramount importance for several reasons. Firstly, its value determines the Higgs boson production rates and decay branching ratios [3]. It is also the value assumed by the experimental collaborations when estimating the acceptances, efficiencies and signal models used in their analyses and to report their measured rates. Knowledge of the Higgs boson mass is therefore mandatory for a coherent test of its coupling structure. Secondly, the Higgs boson mass is one of the inputs in global fits to the measurements of electroweak observables [4]. Knowing its value therefore plays a key role in verifying the internal consistency of the SM, especially through the interplay between the masses of the top quark and the W and Higgs bosons. Finally, the stability of the electroweak vacuum, and thus the fate of our universe, depends on the value of the Higgs boson mass [5]. By measuring m_H , one can infer whether the universe is in a global, and thus stable, minimum-energy state of the Higgs field potential, or in a local metastable one, from which it could decay to the ground state in the future [6].

Measurements of the Higgs boson mass were performed separately by the ATLAS [7] and CMS [8] collaborations using Higgs boson decays to the high-resolution four-lepton (4ℓ , $\ell = e, \mu$) and diphoton ($\gamma\gamma$) final states reconstructed during the first data-taking phase of the LHC (Run 1). The data consisted of 25 fb^{-1} of proton–proton (pp) collisions recorded at centre-of-mass energies $\sqrt{s} = 7$ and 8 TeV in 2011 and 2012. The combination of the ATLAS and CMS results led to a measurement of the Higgs boson mass with an uncertainty of 0.19%, $m_H = 125.09 \pm 0.24 \text{ GeV}$ [9].

Updated measurements of the Higgs boson mass were performed by both experiments using pp collisions collected at $\sqrt{s} = 13$ TeV between 2015 and 2018 during the second data-taking phase of the LHC (Run 2). Using both $H \rightarrow ZZ^* \rightarrow 4\ell$ and $H \rightarrow \gamma\gamma$ decays selected in a partial Run 2 dataset (36 fb^{-1} of pp collisions recorded before 2017), the ATLAS Collaboration measured $m_H = 124.86 \pm 0.27 \text{ GeV}$ [10]. Combined with the ATLAS Run 1 results from Ref. [7], this study led to a Higgs boson mass measurement of $m_H = 124.97 \pm 0.24 \text{ GeV}$. Using a dataset of equivalent size and both the four-lepton and diphoton final states, the CMS Collaboration found $m_H = 125.46 \pm 0.16 \text{ GeV}$ [11], whose combination with the Run 1 results from Ref. [8] led to the most precise determination of m_H to date, with a 0.11% uncertainty: $m_H = 125.38 \pm 0.14 \text{ GeV}$. Recently, the ATLAS Collaboration released an updated measurement of m_H using $H \rightarrow ZZ^* \rightarrow 4\ell$ decays in the full Run 2 dataset [12], consisting of 140 fb^{-1} of pp collisions. The result, $m_H = 124.99 \pm 0.19 \text{ GeV}$, combined with that of the corresponding analysis using Run 1 data, yields a single-channel Higgs boson mass measurement with an uncertainty of 0.14%, $m_H = 124.94 \pm 0.18 \text{ GeV}$.

This Letter reports a measurement of the Higgs boson mass in the diphoton channel using the full Run 2 dataset. Compared with that in Ref. [10], the analysis presented here profits from a larger data sample, a new photon reconstruction algorithm with better energy resolution [13], an improved estimation of the photon energy scale with reduced uncertainties [14], and an optimised event classification strategy. The selected events are required to contain two energetic photons fulfilling strict identification and isolation criteria. The invariant mass ($m_{\gamma\gamma}$) distribution of the selected photon pairs exhibits a peak near m_H , arising from resonant Higgs boson decays, over a smoothly falling distribution from background events mainly due to non-resonant diphoton production. The Higgs boson mass is determined from the position of the peak in data through a profile-likelihood fit to the $m_{\gamma\gamma}$ distribution. Simulated signal and background event samples are used to optimise the analysis criteria, to define the signal and background $m_{\gamma\gamma}$ models used in the fit, and to estimate the impact of the systematic uncertainties in m_H . To increase the sensitivity of the measurement, the selected events are classified into mutually exclusive categories with different diphoton invariant mass resolutions and signal-to-background ratios which are analysed simultaneously. Finally, a combination with the ATLAS Run 1 measurement [9] is performed.

The rest of the Letter is organised as follows. The ATLAS detector is described briefly in Section 2. The data and simulated event samples used in the analysis are summarised in Section 3. The photon reconstruction and the event selection and classification are discussed in Section 4. The statistical tools used in the measurement and the methods used to assess the systematic uncertainties are presented in Sections 5 and 6, leading to the results described in Section 7. The conclusions of this study are summarised in Section 8.

2 The ATLAS detector

The ATLAS experiment [15] at the LHC is a multipurpose particle detector with a forward–backward symmetric cylindrical geometry and a near 4π coverage in solid angle.¹ It consists of an inner tracking detector surrounded by a thin superconducting solenoid providing a 2 T axial magnetic field, electromagnetic and hadron calorimeters, and a muon spectrometer. The inner tracking detector covers the pseudorapidity

¹ ATLAS uses a right-handed coordinate system with its origin at the nominal interaction point (IP) in the centre of the detector and the z -axis along the beam pipe. The x -axis points from the IP to the centre of the LHC ring, and the y -axis points upwards. Cylindrical coordinates (r, ϕ) are used in the transverse plane, ϕ being the azimuthal angle around the z -axis. The pseudorapidity is defined in terms of the polar angle θ as $\eta = -\ln \tan(\theta/2)$. Angular distance is measured in units of $\Delta R \equiv \sqrt{(\Delta\eta)^2 + (\Delta\phi)^2}$. The transverse energy is defined as $E_T = E \sin(\theta)$.

range $|\eta| < 2.5$. It consists of silicon pixel, silicon microstrip, and transition radiation tracking detectors. Lead/liquid-argon (LAr) sampling calorimeters provide electromagnetic (EM) energy measurements with high granularity. A steel/scintillator-tile hadron calorimeter covers the central pseudorapidity range ($|\eta| < 1.7$). The endcap and forward regions are instrumented with LAr calorimeters for both the EM and hadronic energy measurements up to $|\eta| = 4.9$. The muon spectrometer surrounds the calorimeters and is based on three large superconducting air-core toroidal magnets with eight coils each. The field integral of the toroids ranges between 2.0 and 6.0 T m across most of the detector. The muon spectrometer includes a system of precision chambers for tracking and fast detectors for triggering.

A two-level trigger system is used to select events. The first-level trigger is implemented in hardware and uses a subset of the detector information to accept events at a rate below 100 kHz. This is followed by a software-based trigger that reduces the accepted event rate to 1 kHz on average depending on the data-taking conditions.

An extensive software suite [16] is used in data simulation, in the reconstruction and analysis of real and simulated data, in detector operations, and in the trigger and data acquisition systems of the experiment.

3 Data and simulation samples

3.1 Data

The measurement uses the full pp collision dataset collected at $\sqrt{s} = 13$ TeV by the ATLAS detector during Run 2 of the LHC. Events were recorded using unprescaled diphoton and single-photon triggers [17]. The photon transverse momentum thresholds were 35 GeV and 25 GeV for the diphoton triggers throughout the whole of Run 2, and 120 (140) GeV for single-photon triggers in 2015–2016 (2017–2018). Shower-shape requirements looser than those used in the offline analysis were applied to the photon candidates at the trigger level. The integrated luminosity of the dataset after trigger and data-quality requirements [18] is $140.1 \pm 1.2 \text{ fb}^{-1}$ [19, 20]. The efficiency of the trigger system for signal events passing the full selection is close to 100% [17].

3.2 Simulation samples

Monte Carlo (MC) simulated event samples of Higgs bosons produced by pp collisions and decaying into diphotons, as well as samples of the main background processes for the same final state, were produced with the set-up described in Ref. [21]. Simulated hard-scattering events were overlaid with simulated inelastic proton–proton events generated with PYTHIA 8.1 [22], to model the effect of multiple ‘pile-up’ interactions in the same and neighbouring bunch crossings.

Signal samples were produced for the main Higgs boson production modes: gluon–gluon fusion (ggF), vector-boson fusion (VBF), and associated production with a vector boson (VH , $V = W, Z$), a top-quark pair ($t\bar{t}H$), a bottom-quark pair ($b\bar{b}H$) or a single top quark (tH). Signal event samples were produced with either the POWHEG BOX [23] or (for tH only) MADGRAPH5_AMC@NLO [24] event generator, using matrix element calculations at the highest available order of accuracy in the strong coupling constant α_s : next-to-next-to-leading order (NNLO) for ggF, next-to-leading order (NLO) for VBF, WH , $q\bar{q} \rightarrow ZH$, $t\bar{t}H$, $b\bar{b}H$ and tH , and leading order (LO) for $gg \rightarrow ZH$. The event generators were interfaced to PYTHIA 8.2 [25] for the modelling of the parton shower and the underlying event. In the analysis the

samples are normalised to the integrated luminosity of the data, using state-of-the-art Standard Model calculations for the Higgs boson production cross-sections and branching ratios at the hypothesised Higgs boson mass [3]. The generated signal samples were passed through a detailed simulation of the response of the ATLAS detector [26] based on GEANT4 [27].

The nominal signal samples were generated assuming a Higgs boson mass of 125 GeV. The Higgs boson width Γ in all signal samples was set to the SM prediction for $m_H = 125$ GeV, $\Gamma = 4.07$ MeV, which is much narrower than the experimental resolution. Systematic uncertainties related to the modelling of the parton shower are studied with alternative samples produced with the same matrix-element generator as used for the nominal ones but with the HERWIG 7.1.3 parton shower algorithm [28]. The parameterisations of the expected signal yields and diphoton invariant mass distributions as a function of the Higgs boson mass are obtained by interpolation between results from signal samples with m_H set to 110, 122, 123, 124, 125, 126, 127, 130 or 140 GeV, as described in Section 5. The same set-up as that for the nominal samples was used.

Background events from non-resonant $pp \rightarrow \gamma\gamma + n$ parton ($n \geq 0$) production were also simulated, using the SHERPA 2.2.4 event generator [29] with NLO-accurate matrix elements for up to one parton, and leading-order (LO) accurate matrix elements for up to three partons. Due to its large size, the $pp \rightarrow \gamma\gamma$ sample was processed by a fast simulation of the ATLAS detector [30], based on a parameterisation of the response of the calorimeter. Since the diphoton background is estimated from the sidebands in the diphoton invariant mass distribution in data, the background simulation is only used to select the background model and the systematic uncertainty associated with this choice, and for this the fast simulation was found to be sufficiently accurate.

The effect of interference between resonant signal production and non-resonant background diphoton production is studied using samples of simulated diphoton events including contributions from both processes (produced by either the gg or qg partonic channels) and their interference. The accuracy of the calculations is NLO for the gg -interference and LO for the qg -interference samples. The events were generated using SHERPA 2.2.11 and passed through the GEANT4 detector simulation.

4 Event selection and classification

The event reconstruction and selection closely resemble those used in the latest ATLAS measurement of Higgs boson production cross-sections using the diphoton channel and the full Run 2 dataset [21]. The main differences are the use of an updated photon energy calibration [14] with reduced systematic uncertainties, and the classification of events into categories that are optimised to minimise the uncertainty in the measured Higgs boson mass rather than in the Higgs boson production cross-sections.

Compared with the previous mass measurement [10], which used photon candidates reconstructed from a fixed-size cluster of energy deposits in the electromagnetic calorimeter identified by a sliding-window algorithm, this measurement relies on photon candidates that are reconstructed from dynamic, variable-size clusters, called superclusters. The main advantages of this algorithm are improvements in the reconstruction efficiency and energy measurement of converted photons ($\gamma \rightarrow e^+e^-$), and a lower rate of misclassifying unconverted photons as converted photon candidates [13].

The photon energy is determined from the signals due to energy deposited in the electromagnetic calorimeter, after applying the calibration scheme detailed in Ref. [14]. The photon direction is calculated from the positions of the supercluster and the pp collision vertex that is chosen from among the reconstructed

primary vertex candidates by a neural-network (NN) algorithm [31]. The NN inputs are the directions of the two p_T -leading photon candidates in the event, determined only from the conversion vertices and the longitudinal sampling of the calorimeter, and vertex candidate information such as the transverse momenta and directions of the associated tracks.

The selection retains events with at least two photon candidates with pseudorapidity in the range $|\eta| < 1.37$ or $1.52 < |\eta| < 2.37$, meeting *tight* identification and *loose* isolation criteria [13], matched to the online photon candidates that passed the trigger selection. Events are kept if the p_T -leading and p_T -subleading photon candidates have invariant mass $m_{\gamma\gamma}$ in the range 105–160 GeV and transverse momenta that exceed 0.35 and 0.25 times $m_{\gamma\gamma}$, respectively. When more than two photon candidates pass those requirements, only the p_T -leading and p_T -subleading candidates are considered for further analysis.

About 1.2 million events in the data pass the selection. The expected efficiency for the signal for $m_H = 125$ GeV is close to 36%, leading to an expected signal yield of about 6200 events.

To increase the precision of the mass measurement, the selected events are classified into 14 categories with different signal-to-background ratios, diphoton invariant mass resolutions and photon energy scale uncertainties. The observables and the thresholds used to define the categories are optimised by minimising the expected total Higgs boson mass uncertainty for $m_H = 125.09$ GeV using a simplified version of the maximum-likelihood fit described in the next section, including the statistical uncertainties and the dominant systematic uncertainties from the photon energy scale calibration. The final choice of observables and thresholds for the categories used in the measurement is the following:

- The number of reconstructed converted photon candidates: events with no photon conversion candidates ('U'-type events) are considered separately from events with one or two $\gamma \rightarrow e^+e^-$ candidates ('C'-type events).
- The absolute value of the pseudorapidity $|\eta_{S2}|$ of each of the two energy clusters reconstructed in the electromagnetic calorimeter and associated with the photon candidates. The pseudorapidity η_{S2} is determined from the position of the barycentre of the cluster in the second sampling layer of the calorimeter and from the origin of the ATLAS coordinate system. Both the U-type and C-type events are separated into three subsamples: 'central barrel' (both photons have $|\eta_{S2}| < 0.8$), 'outer-barrel' (both photons have $|\eta_{S2}| < 1.37$ and at least one of these has $|\eta_{S2}| \geq 0.8$), and 'endcap' (at least one photon has $1.52 \leq |\eta_{S2}| < 2.37$).
- The magnitude $p_{Tt}^{\gamma\gamma} = |\vec{p}_T^{\gamma\gamma} \times \hat{t}|$ of the component of the diphoton transverse momentum that is orthogonal to the thrust axis, defined as $\hat{t} = (\vec{p}_T^{\gamma 1} - \vec{p}_T^{\gamma 2}) / |\vec{p}_T^{\gamma 1} - \vec{p}_T^{\gamma 2}|$. Low ($p_{Tt}^{\gamma\gamma} < 70$ GeV), medium ($70 \text{ GeV} < p_{Tt}^{\gamma\gamma} < 130$ GeV) and high ($p_{Tt}^{\gamma\gamma} > 130$ GeV) $p_{Tt}^{\gamma\gamma}$ categories are defined for U-type and C-type central-barrel and outer-barrel events.

For each category, the narrowest diphoton invariant mass window, with half-width denoted by $\sigma_{90}^{\gamma\gamma}$, containing 90% of the signal events is listed in Table 1. The expected signal (S_{90}) and background (B_{90}) yields in each category in that interval are also reported, where B_{90} is determined from the integral of an exponentiated second-order polynomial function fitted to the data $m_{\gamma\gamma}$ distribution after excluding the range $120 < m_{\gamma\gamma} < 130$ GeV from the interval. The table also indicates the expected fraction of signal events $f_{90} = S_{90} / (S_{90} + B_{90})$, and the signal significance $Z_{90} = \sqrt{2 [(S_{90} + B_{90}) \ln(1 + S_{90}/B_{90}) - S_{90}]}$ [32].

The invariant mass resolution $\sigma_{90}^{\gamma\gamma}$ for C-type events is 10%–20% worse than for U-type events, due to asymmetric $\gamma \rightarrow e^+e^-$ conversions producing a low-energy electron or positron, and to bremsstrahlung photons emitted by the e^+e^- pair. In both cases, such soft electrons, positrons or bremsstrahlung photons

Table 1: The expected signal (S_{90}) and background (B_{90}) yields, the signal yield as a percentage of the total (f_{90}), and the signal significance (Z_{90}) in a diphoton invariant mass window whose half-width $\sigma_{90}^{\gamma\gamma}$ is chosen in such a way that it is the narrowest interval containing 90% of signal events. All quantities are given for each analysis category and for the inclusive case.

Category	$\sigma_{90}^{\gamma\gamma}$ [GeV]	S_{90}	B_{90}	f_{90} [%]	Z_{90}
U, Central-barrel, high $p_{\text{Tt}}^{\gamma\gamma}$	1.88	42	65	39.1	4.7
U, Central-barrel, medium $p_{\text{Tt}}^{\gamma\gamma}$	2.34	102	559	15.4	4.2
U, Central-barrel, low $p_{\text{Tt}}^{\gamma\gamma}$	2.63	837	13226	6.0	7.2
U, Outer-barrel, high $p_{\text{Tt}}^{\gamma\gamma}$	2.16	31	83	27.4	3.3
U, Outer-barrel, medium $p_{\text{Tt}}^{\gamma\gamma}$	2.63	108	981	9.9	3.4
U, Outer-barrel, low $p_{\text{Tt}}^{\gamma\gamma}$	3.00	869	22919	3.7	5.7
U, Endcap	3.33	759	29383	2.5	4.4
C, Central-barrel, high $p_{\text{Tt}}^{\gamma\gamma}$	2.10	26	44	37.3	3.6
C, Central-barrel, medium $p_{\text{Tt}}^{\gamma\gamma}$	2.62	62	389	13.8	3.1
C, Central-barrel, low $p_{\text{Tt}}^{\gamma\gamma}$	3.00	508	9726	5.0	5.1
C, Outer-barrel, high $p_{\text{Tt}}^{\gamma\gamma}$	2.56	34	103	25.0	3.2
C, Outer-barrel, medium $p_{\text{Tt}}^{\gamma\gamma}$	3.20	114	1353	7.8	3.1
C, Outer-barrel, low $p_{\text{Tt}}^{\gamma\gamma}$	3.71	914	30121	2.9	5.2
C, Endcap	4.04	1249	52160	2.3	5.5
Inclusive	3.32	5653	128774	4.2	15.6

can escape the supercluster and the calibration procedure may not be fully efficient in recovering the energy of the original photon. The resolution is 6%–20% better in the central-barrel categories than in the corresponding outer-barrel categories, due to the smaller amount of material upstream of the electromagnetic calorimeter in the central region of the detector. Events with high $p_{\text{Tt}}^{\gamma\gamma}$ have about 15%–20% (30%) better $m_{\gamma\gamma}$ resolution than events with medium (low) $p_{\text{Tt}}^{\gamma\gamma}$, due to poorer photon energy resolution at lower photon transverse momentum. The signal fraction f_{90} also depends on the same quantities: it is larger for U-type events and central-barrel events, and increases with $p_{\text{Tt}}^{\gamma\gamma}$ since the main background process, continuum diphoton production arising mostly from t -channel $q\bar{q} \rightarrow \gamma\gamma$ and $gg \rightarrow \gamma\gamma$ scattering, has a softer $p_{\text{Tt}}^{\gamma\gamma}$ spectrum than the signal. The photon energy scale uncertainty is smaller for C-type events and central-barrel events than for U-type events and outer-barrel or endcap events; it increases with $p_{\text{Tt}}^{\gamma\gamma}$ due to uncertainties in the linearity of the response and in the extrapolation to photons in the energy scale calibration, which is mainly determined using electron and positron candidates with relatively low transverse momentum from $Z \rightarrow e^+e^-$ decays.

The chosen categorisation reduces the expected uncertainty in m_H from statistical and photon energy scale systematic uncertainties by about 17% compared with a measurement based on the inclusive sample passing the event selection, and by 6% compared with the use of the event classification strategy in Ref. [10]. Compared with the 101 event categories developed in Ref. [21] for the measurement of the Higgs boson production-mode cross-sections times branching ratio to diphotons using the same dataset, the 14 categories used in this analysis lead to a small increase (+3%) in the expected statistical uncertainty and to a larger decrease (−14%) in the systematic uncertainty of m_H , yielding an overall expected decrease (−3%) in the total uncertainty.

5 Mass measurement procedure

The Higgs boson mass m_H is measured using the statistical methods described in Ref. [10]. The diphoton invariant mass distribution of the data is used to define a likelihood function L depending on m_H and on additional parameters θ describing the signal and background normalisations, their $m_{\gamma\gamma}$ models, and corresponding systematic uncertainties. The profile likelihood ratio [32, 33] is then:

$$\Lambda(m_H) = \frac{L(m_H, \hat{\theta}(m_H))}{L(\hat{m}_H, \hat{\theta})}, \quad (1)$$

where $\hat{\theta}$ and \hat{m}_H denote the values of the parameters that maximise the likelihood function L , while $\hat{\theta}(m_H)$ represent the values of the parameters θ that maximise L for a given value of the parameter m_H . A numerical fit procedure determines the central value \hat{m}_H of the measurement and its 68% confidence interval, defined by all values of m_H for which $-2 \ln \Lambda(m_H) < 1$. The fit uses the event counts in 25-MeV-wide bins of the $m_{\gamma\gamma}$ distribution in each category.

The likelihood function L is computed from the product of individual likelihood functions for the observed diphoton invariant mass spectra in each category and distributions representing auxiliary measurements that constrain the nuisance parameters associated with the systematic uncertainties. The model assumes that the observed distribution arises from the sum of a signal and a background component, whose shape and normalisation are inferred from the data themselves, with some input from the simulation.

The $m_{\gamma\gamma}$ distribution of the simulated signal in each category is found to be properly described, for any value of the Higgs boson mass in the range [110, 140] GeV, by a double-sided Crystal Ball [34] probability density function, i.e. a function with a Gaussian core and power-law tails. The parameters (α_{\pm}, n_{\pm}) describing the tails of the model do not depend on m_H , while the parameters μ_{CB} and σ_{CB} describing the peak position and the resolution of the core Gaussian component scale linearly with m_H , $\mu_{\text{CB}} = m_H + a_{\mu} + b_{\mu}(m_H - 125 \text{ GeV})$ and $\sigma_{\text{CB}} = a_{\sigma} + b_{\sigma}(m_H - 125 \text{ GeV})$. The nominal values of the parameters a_{μ} , b_{μ} , a_{σ} , b_{σ} , α_{\pm} and n_{\pm} in each category are determined by a simultaneous fit to the simulated diphoton invariant mass spectra in that category for different m_H hypotheses. As a cross-check, the fit is repeated after removing the $m_H = 125 \text{ GeV}$ distribution from the input and new values of the a_{μ} , b_{μ} , a_{σ} , b_{σ} , α_{\pm} and n_{\pm} parameters are obtained. The signal model for $m_H = 125 \text{ GeV}$ predicted by this parameterisation is then compared with the model determined from a single fit, with a Crystal-Ball lineshape with floating μ_{CB} , σ_{CB} , α_{\pm} and n_{\pm} parameters, to the $m_H = 125 \text{ GeV}$ simulated signal events. Good agreement is observed. The nominal signal models for the categories with the best and worst expected resolutions for a Higgs boson mass $m_H = 125 \text{ GeV}$ are shown in Figure 1.

The normalisations of the signal, one for each category c , are free parameters of the fit and are expressed as the product of a per-category signal-strength factor μ_c and the expected number S_c of Higgs boson events in the same analysis region. The expected signal yield S_c is determined from the integrated luminosity, the SM values of the Higgs boson cross-section and $H \rightarrow \gamma\gamma$ branching ratio, and the simulation-predicted event selection efficiency in that category. The dependence of S_c on m_H in each category c is modelled with a second-order polynomial whose parameters are determined by a fit to the expected yields in that category, calculated for nine discrete values of m_H between 110 and 140 GeV using the simulated signal samples described in Section 3.

The background $m_{\gamma\gamma}$ distribution in each category is represented by either an exponential function, a power-law function or an exponentiated second-order polynomial. The background model is chosen in

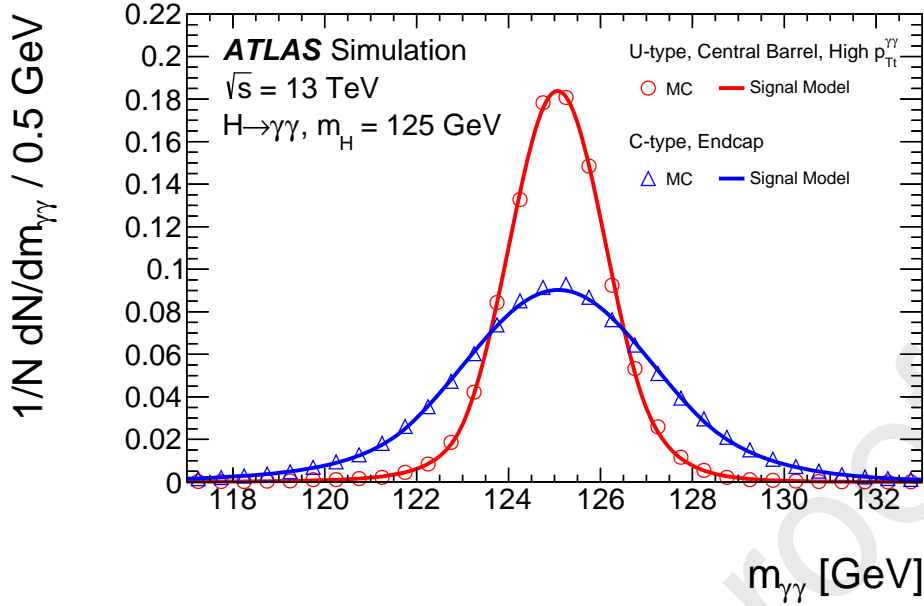


Figure 1: Invariant mass distributions of simulated $H \rightarrow \gamma\gamma$ events reconstructed in the categories with the best (U-type, central-barrel, high- $p_{T}^{\gamma\gamma}$: open circles) and the worst (C-type, endcap: open squares) experimental resolutions. The signal model derived from a fit of the simulated events is superimposed (solid lines).

an empirical way [21], using the results obtained by fitting the diphoton invariant mass distribution of a background template with models with free parameters for the signal and background yields. The background template is obtained by summing the $m_{\gamma\gamma}$ distributions of simulated non-resonant diphoton events and data samples enriched in photon+jet and dijet events. The photon+jet and dijet enriched samples are obtained using a selection similar to that in the previous section, the exception being that one or both photon candidates must fail the nominal identification and isolation requirements while passing looser ones. The three distributions are normalised to the yields of the respective contributions estimated in situ. Among all considered background models whose χ^2 probability is greater than 1% when fitted to the background template, and for which the fitted signal yield (the ‘spurious signal’) is less than 10% of the expected signal yield, the one with the fewest degrees of freedom is selected. A value of 10% is chosen for the threshold so that the spurious signal, considered as a systematic uncertainty in the signal yield, is small compared to the statistical uncertainty. The background yield in each category and the parameters describing the shape of the background model are free parameters of the likelihood function.

Systematic uncertainties and their correlations are modelled by including, among the parameters θ , nuisance parameters described by likelihood functions associated with estimates of the corresponding effects. The statistical uncertainty of m_H is estimated by determining the confidence interval when all nuisance parameters associated with systematic uncertainties are fixed to their best-fit values, and all other parameters are left unconstrained. The total systematic uncertainty is estimated as the square root of the difference of the squares of the total uncertainty and the statistical uncertainty. Similarly, the contribution from a group of uncertainties is determined from the difference of the squares of the total uncertainty and the uncertainty from a fit in which the associated nuisance parameters are fixed to their best-fit values.

The expected statistical uncertainty of 120 MeV in m_H is a factor of 2.1 less than in the previous measurement [10], due to the present dataset being almost four times larger and improvements in the

photon reconstruction algorithm and event classification.

6 Systematic uncertainties

The main sources of systematic uncertainty in m_H are the uncertainties in the photon energy scale, the uncertainty from the background modelling and the effect of interference between the signal and the $\gamma\gamma$ continuum background. They are described below, together with their expected pre-fit impact on m_H .

The photon energy scale uncertainty is modelled by using 67 independent components. The effect of every component is evaluated for each analysis category by comparing the nominal signal MC diphoton invariant mass distribution with the one obtained by varying the energy of each photon by the uncertainty under study. The shifts induced in the peak parameters μ_{CB} of the Crystal Ball signal models are then included as nuisance parameters in the likelihood function, fully correlated among the categories. The 67 independent sources of uncertainty in the photon energy scale can be classified roughly into four main groups. The first group ($Z \rightarrow e^+e^-$ calibration) is related to the determination of the η -dependent energy scale factors for electrons and positrons from Z boson decays, effectively constraining their energy scale for a transverse energy $E_T \approx 45$ GeV. The second group (E_T -dependent electron energy scale) includes uncertainties in the E_T -dependence of the energy scale from sources such as the calorimeter readout non-linearity, the calorimeter layer intercalibration, and the amount of material upstream of the calorimeter. The third group ($e^\pm \rightarrow \gamma$ extrapolation) includes the uncertainties in the extrapolation of the energy scale from electrons to photons, arising, for instance, from potential mismodelling of differences in lateral shower development between electrons and photons in the calorimeter. Finally, the fourth group (conversion modelling) contains the uncertainties related to the accuracy of the photon conversion modelling in the simulation. Since the simulation-based photon energy calibration [14] is trained and applied separately for unconverted and converted photon candidates, any mismodelling of the conversion reconstruction performance in the simulation may affect the calibrated photon energy scale.

The results presented in this Letter profit from a new auxiliary measurement (*linearity fit*) of the data-to-MC electron energy scale corrections as a function of the electron E_T . In the photon energy scale calibration used in the previous Higgs boson mass measurement [10], only η -dependent energy scale factors were derived from 2015–2016 data. These were obtained by comparing the position of the peak of the invariant mass distribution of e^+e^- pairs from Z boson decays with that predicted by the simulation. The possible E_T -dependence of the data-to-MC energy scale correction was accounted for as a systematic uncertainty, arising from the various sources belonging to the E_T -dependent electron energy scale group, calculated as described in Ref. [35]. The new approach used in Ref. [14] exploits the larger sample of $Z \rightarrow e^+e^-$ decays collected in 2015–2018 to derive residual data-to-MC energy scale factors in bins of electron transverse energy within broad η regions. The measurement of these additional scale factors is used to constrain the E_T -dependent electron energy scale systematic uncertainties. The additional constraints and correlation of the systematic uncertainties from the linearity fit are propagated to the Higgs boson mass measurement by implementing in the likelihood function a multivariate Gaussian constraint term whose covariance is that returned by the linearity fit. The impact of the photon energy scale systematic uncertainties, including the effect of the linearity fit, was found to be independent of m_H for Higgs boson mass values in the range 124–126 GeV, and is expected to be approximately ± 83 MeV (with contributions of 60, 43, 30 and 23 MeV, respectively, from the four individual groups of $Z \rightarrow e^+e^-$ calibration, E_T -dependent electron energy scale, $e^\pm \rightarrow \gamma$ extrapolation and conversion modelling uncertainties). Compared to the results in Ref. [10], the simulation's more accurate description [13] of material upstream of the EM calorimeter and the lower

sensitivity of the new clustering algorithm to the effects of interactions with detector material reduced the associated systematic uncertainty by a factor close to three. In addition, the larger dataset allowed a more precise study of the $e^\pm \rightarrow \gamma$ extrapolation procedure [14], and its impact on the expected m_H uncertainty is reduced by a factor larger than three. Furthermore, the contribution of the E_T -dependent electron energy scale uncertainties to the total expected m_H uncertainty has been reduced by a factor of two thanks to more precise dedicated measurements. Finally, the linearity fit constrains the expected uncertainty in the Higgs boson mass from the group of E_T -dependent energy scale uncertainties by a further factor of four.

The effect of interference between the $gg \rightarrow H \rightarrow \gamma\gamma$ signal and the $gg \rightarrow \gamma\gamma$ continuum background and between $gq \rightarrow H \rightarrow \gamma\gamma$ and $gq \rightarrow \gamma\gamma$ is not included in the simulated event samples used to study the nominal signal model. In the Standard Model, this interference is expected to change the signal cross-section by 1%–2% [36] and to shift the position of the peak in the diphoton invariant mass distribution by a few tens of MeV [37]. The size of this effect is treated as a systematic uncertainty, which is quantified by fitting the nominal signal-plus-background model to the sum of the $m_{\gamma\gamma}$ distributions predicted by the nominal signal and background models and the $m_{\gamma\gamma}$ distribution arising from such interference in simulated events. The relative differences between the nominal Higgs boson mass and the fitted mass in the various analysis categories are included in the likelihood function as a single nuisance parameter affecting the 14 categories coherently. The impact of the interference term on the determination of m_H is expected to be approximately ± 24 MeV.

The effect of a possible bias in the measured m_H value, due to mismodelling of the continuum background $m_{\gamma\gamma}$ distribution, is evaluated by fitting the signal-plus-background model to the sum of the $m_{\gamma\gamma}$ distribution of the background template described in the previous section and the $m_{\gamma\gamma}$ distribution predicted by the signal model for $m_H = 125$ GeV. The relative differences between the nominal Higgs boson mass and the fitted mass in the various analysis categories are then included in the likelihood function as 14 additional uncorrelated nuisance parameters, one per category. The impact of the background modelling uncertainty on the measurement of m_H is expected to be approximately ± 18 MeV.

The systematic uncertainty related to the selection of the diphoton production vertex is evaluated in a $Z \rightarrow e^+e^-$ control sample. The directions of the selected electrons and positrons and thus their invariant mass are calculated using either the primary vertex candidate with the largest sum of the squared transverse momenta of the tracks associated to the vertex (which includes also the e^\pm tracks), or the primary vertex selected by the NN algorithm described in Section 4, where the electron and positron tracks are ignored. The separation between the peak positions of the two e^+e^- invariant mass distributions is evaluated separately in data and simulation. The maximum difference (5 MeV) between the separation observed in data and that observed in the simulation is taken as an additional systematic uncertainty in m_H .

Uncertainties from the chosen parameterisation of the nominal signal model are propagated to the final result by including 14 additional uncorrelated nuisance parameters in the likelihood function. They are determined by fitting the nominal signal-plus-background model to the sum of the $m_{\gamma\gamma}$ distribution of simulated $m_H = 125$ GeV signal events and that predicted by the nominal background model. The impact of the signal modelling uncertainty on the measurement of m_H is expected to be approximately ± 5 MeV.

The effect of the photon energy resolution uncertainty is included in the signal model as five nuisance parameters that affect the resolution parameter σ_{CB} of the Crystal Ball function and are treated as being correlated among categories. The impact of the five independent sources of photon energy resolution uncertainty is evaluated by comparing the nominal signal invariant mass distribution in each category with the ones obtained by varying the energy resolution of each photon according to its uncertainties. The sum in quadrature of the different components of the photon energy resolution uncertainty ranges from 4.5% for

C-type, outer-barrel, low- $p_{\text{T}}^{\gamma\gamma}$ events to 17% for U-type, central-barrel, high- $p_{\text{T}}^{\gamma\gamma}$ events. The impact of the photon energy resolution uncertainty on m_H is expected to be approximately ± 3 MeV.

Yield uncertainties from the Higgs boson branching ratio to diphotons and the integrated luminosity of the data, and uncertainties in the migrations of events between categories, from various experimental and theoretical sources, are included in the model. Experimental uncertainties in the efficiency of photon conversion reconstruction, photon identification, photon isolation and the photon triggers, as well as in the impact of the simulation's modelling of pile-up are considered. Theoretical uncertainties that are taken into account are those in the signal production cross-sections, in the modelling of the underlying event and parton shower, in the value of the strong coupling constant and in the parton distribution functions of the proton. All the uncertainties described in this paragraph are included in the fit, although their expected impact on the measurement of m_H was found to be below 1 MeV.

In summary, compared to the previous publication [10] based on 36 fb^{-1} of ATLAS Run 2 data, the improvements in the photon energy calibration [14] and the optimised event classification lead to an expected fourfold reduction of the dominant systematic uncertainty in m_H (from the photon energy scale and resolution), from 320 MeV to 80 MeV, and a similar reduction of the total expected systematic uncertainty, from 330 MeV to 90 MeV.

7 Results

The $m_{\gamma\gamma}$ distribution of the data, overlaid with the sum of the signal and background models corresponding to the maximum-likelihood estimates of the parameters of the likelihood function, is shown in Figure 2. All event categories are included. For illustration purposes, events in each category are weighted by a factor $\ln(1 + S_{90}^{\text{obs}}/B_{90}^{\text{obs}})$, where S_{90}^{obs} and B_{90}^{obs} are the fitted signal and background yields in the smallest $m_{\gamma\gamma}$ interval containing 90% of the signal.

The profile likelihood ratio as a function of m_H is shown in Figure 3(a). The value of the Higgs boson mass determined by fitting the profile likelihood ratio in Eq. (1) to the diphoton invariant mass distribution in data is:

$$m_H = 125.17 \pm 0.11(\text{stat.}) \pm 0.09(\text{syst.}) \text{ GeV} = 125.17 \pm 0.14 \text{ GeV}.$$

The statistical and systematic uncertainties are in good agreement with the values of 120 MeV and 90 MeV expected for a SM Higgs boson with the observed mass. The main sources of systematic uncertainty and their impact on the measurement are summarised in Table 2.

The signal strength μ_c in each category c is compatible with the SM prediction $\mu_c = 1$, with the largest difference being 2.2 standard deviations (σ) for the C-type, central-barrel, medium- $p_{\text{T}}^{\gamma\gamma}$ category. The global significance of this difference, taking into account a trial factor of 14, is less than 1σ . The best-fit m_H values for the individual categories are in good agreement with each other, with a global p -value of 8%. If the same signal strength μ is used for each category, the central value of m_H is shifted by -35 MeV, and the fitted value of μ is in agreement with the SM prediction within 1.4 standard deviations. If the signal $m_{\gamma\gamma}$ model is modified to account for the expected shift induced by interference with non-resonant background diphoton production, the measured value of the Higgs boson mass is increased by approximately 26 MeV.

The present measurement is combined with the previous one, $m_H = 126.02 \pm 0.43(\text{stat.}) \pm 0.27(\text{syst.}) \text{ GeV}$, obtained by ATLAS in the diphoton channel using 25 fb^{-1} of proton–proton collisions recorded at $\sqrt{s} = 7$ and 8 TeV during Run 1 of the LHC in 2011–2012 [9]. The combination of ATLAS Run 1 and Run 2

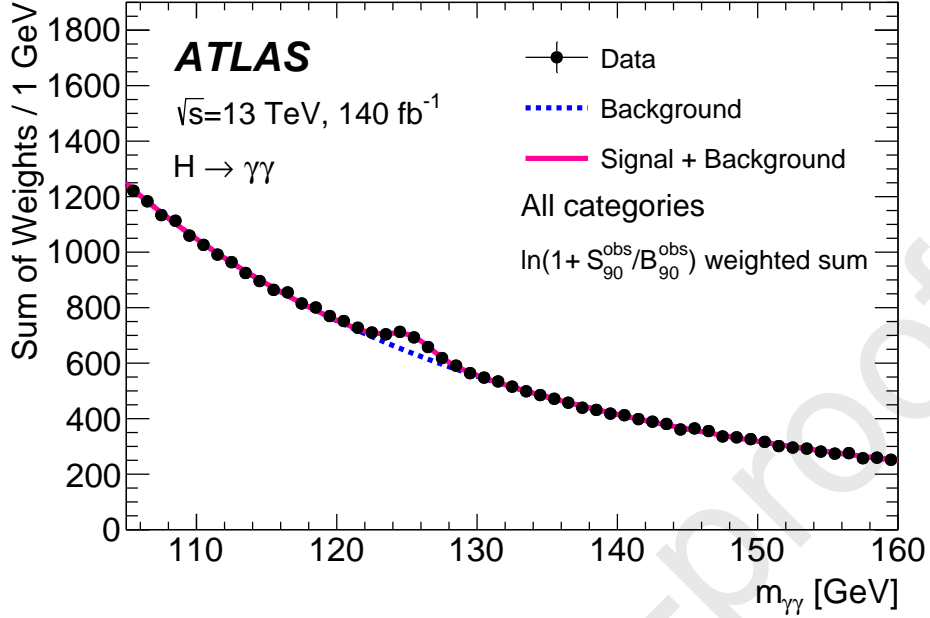


Figure 2: Diphoton invariant mass distribution of all selected data events (black dots with error bars), overlaid with the result of the fit (solid red line). For both the data and the fit, each category is weighted by a factor $\ln(1 + S_{90}^{\text{obs}}/B_{90}^{\text{obs}})$, where S_{90}^{obs} and B_{90}^{obs} are the fitted signal and background yields in the smallest $m_{\gamma\gamma}$ interval containing 90% of the expected signal. The dotted line describes the background component of the model.

Table 2: Estimated impact of the main sources of systematic uncertainty on the m_H measurement with Run 2 data.

Source	Impact [MeV]
Photon energy scale	83
$Z \rightarrow e^+e^-$ calibration	59
E_T -dependent electron energy scale	44
$e^\pm \rightarrow \gamma$ extrapolation	30
Conversion modelling	24
Signal-background interference	26
Resolution	15
Background model	14
Selection of the diphoton production vertex	5
Signal model	1
Total	90

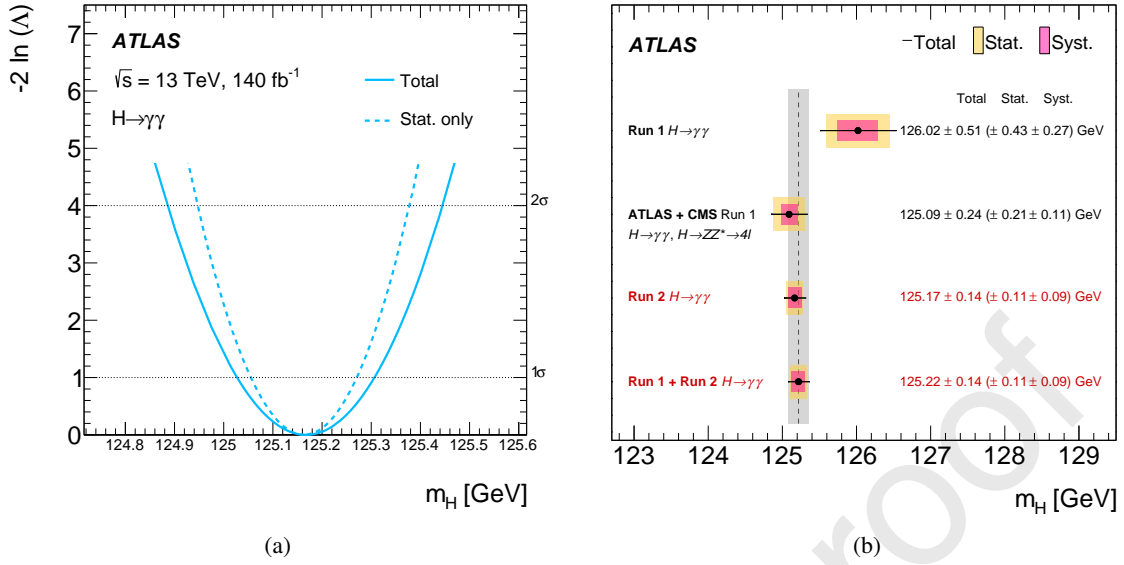


Figure 3: (a) Value of $-2 \ln \Lambda$ as a function of m_H for the combined fit to all $H \rightarrow \gamma\gamma$ categories. The intersections of the $-2 \ln \Lambda$ curve with the horizontal lines labelled 1σ and 2σ provide the 68.3% and 95.5% confidence intervals. (b) Summary of the Higgs boson mass measurements from the analysis of $H \rightarrow \gamma\gamma$ decays in ATLAS Run 2 data and combined Run 1 + Run 2 data presented in this Letter, compared with the combined Run 1 ATLAS result in the diphoton channel and with the Run 1 measurement by ATLAS and CMS [9] combining the diphoton and four-lepton channels. The statistical, systematic and total uncertainties are indicated with horizontal yellow-shaded bands, pink-shaded bands and black error bars, respectively. The vertical dashed line and grey shaded band around it indicate the central value and total uncertainty of the $H \rightarrow \gamma\gamma$ ATLAS Run 1 + Run 2 measurement.

results is performed by simultaneously fitting a single m_H parameter to the two datasets. The nominal model including the 14 signal strengths μ_c of the reconstructed categories is used for the Run 2 dataset, while two separate signal strengths, one each for production processes involving Higgs boson couplings to either fermions or vector bosons, are used for the Run 1 dataset. All 16 signal-strength parameters are profiled in the combined fit for m_H . Almost all the nuisance parameters, especially the E_T -dependent photon energy scale parameters affected by the linearity measurement and the parameters describing the extrapolation of the energy scale from electrons to photons, are assumed to be uncorrelated between the two measurements because of differences in the reconstruction algorithms and in the calibration procedures and control samples. The $Z \rightarrow e^+e^-$ scale uncertainties and some of the resolution uncertainties, estimated in the same way for the two measurements, are treated as being fully correlated between the two data-taking periods. The combination with the Run 1 ATLAS measurement in the diphoton channel produces a small shift (+50 MeV) of the central value and a slight reduction (<10 MeV) of the statistical uncertainty, leading to:

$$m_H = 125.22 \pm 0.11(\text{stat.}) \pm 0.09(\text{syst.}) \text{ GeV} = 125.22 \pm 0.14 \text{ GeV}.$$

The individual ATLAS Run 1 and Run 2 measurements in the diphoton channel and their combination are shown in Figure 3(b), together with the ATLAS+CMS Run 1 measurement [9] using $H \rightarrow \gamma\gamma$ and $H \rightarrow 4\ell$ decays.

8 Conclusion

A measurement of the Higgs boson mass in the diphoton channel has been performed using the Run 2 pp collision data recorded by the ATLAS experiment at the CERN Large Hadron Collider at a centre-of-mass energy of 13 TeV, corresponding to an integrated luminosity of 140 fb^{-1} . Compared to a previous measurement in the same decay channel, which was based on a four times smaller dataset at the same energy, this measurement has a systematic (total) uncertainty that is reduced by a factor close to four (three). The reduction in systematic uncertainty is mainly due to an improved photon energy scale calibration, with better energy resolution, and smaller E_T -dependent and $e^\pm \rightarrow \gamma$ extrapolation uncertainties.

The Higgs boson mass is measured to be $m_H = 125.17 \pm 0.14 \text{ GeV}$. Combined with the Run 1 ATLAS result in the same decay channel, it yields a value $m_H = 125.22 \pm 0.14 \text{ GeV}$. With an uncertainty of 1.1 per mille, this is currently the most precise measurement of the Higgs boson mass from a single channel.

Acknowledgements

We thank CERN for the very successful operation of the LHC, as well as the support staff from our institutions without whom ATLAS could not be operated efficiently.

We acknowledge the support of ANPCyT, Argentina; YerPhI, Armenia; ARC, Australia; BMWFW and FWF, Austria; ANAS, Azerbaijan; CNPq and FAPESP, Brazil; NSERC, NRC and CFI, Canada; CERN; ANID, Chile; CAS, MOST and NSFC, China; Minciencias, Colombia; MEYS CR, Czech Republic; DNRF and DNSRC, Denmark; IN2P3-CNRS and CEA-DRF/IRFU, France; SRNSFG, Georgia; BMBF, HGF and MPG, Germany; GSRI, Greece; RGC and Hong Kong SAR, China; ISF and Benoziyo Center, Israel; INFN, Italy; MEXT and JSPS, Japan; CNRST, Morocco; NWO, Netherlands; RCN, Norway; MEiN, Poland; FCT, Portugal; MNE/IFA, Romania; MESTD, Serbia; MSSR, Slovakia; ARRS and MIZŠ, Slovenia; DSI/NRF, South Africa; MICINN, Spain; SRC and Wallenberg Foundation, Sweden; SERI, SNSF and Cantons of Bern and Geneva, Switzerland; MOST, Taiwan; TENMAK, Türkiye; STFC, United Kingdom; DOE and NSF, United States of America. In addition, individual groups and members have received support from BCKDF, CANARIE, Compute Canada and CRC, Canada; PRIMUS 21/SCI/017 and UNCE SCI/013, Czech Republic; COST, ERC, ERDF, Horizon 2020 and Marie Skłodowska-Curie Actions, European Union; Investissements d'Avenir Labex, Investissements d'Avenir Idex and ANR, France; DFG and AvH Foundation, Germany; Herakleitos, Thales and Aristeia programmes co-financed by EU-ESF and the Greek NSRF, Greece; BSF-NSF and MINERVA, Israel; Norwegian Financial Mechanism 2014-2021, Norway; NCN and NAWA, Poland; La Caixa Banking Foundation, CERCA Programme Generalitat de Catalunya and PROMETEO and GenT Programmes Generalitat Valenciana, Spain; Göran Gustafssons Stiftelse, Sweden; The Royal Society and Leverhulme Trust, United Kingdom.

The crucial computing support from all WLCG partners is acknowledged gratefully, in particular from CERN, the ATLAS Tier-1 facilities at TRIUMF (Canada), NDGF (Denmark, Norway, Sweden), CC-IN2P3 (France), KIT/GridKA (Germany), INFN-CNAF (Italy), NL-T1 (Netherlands), PIC (Spain), ASGC (Taiwan), RAL (UK) and BNL (USA), the Tier-2 facilities worldwide and large non-WLCG resource providers. Major contributors of computing resources are listed in Ref. [38].

References

- [1] ATLAS Collaboration, *Observation of a new particle in the search for the Standard Model Higgs boson with the ATLAS detector at the LHC*, *Phys. Lett. B* **716** (2012) 1, arXiv: 1207.7214 [hep-ex].
- [2] CMS Collaboration, *Observation of a new boson at a mass of 125 GeV with the CMS experiment at the LHC*, *Phys. Lett. B* **716** (2012) 30, arXiv: 1207.7235 [hep-ex].
- [3] D. de Florian et al., *Handbook of LHC Higgs Cross Sections: 4. Deciphering the Nature of the Higgs Sector*, (2016), arXiv: 1610.07922 [hep-ph].
- [4] J. Haller et al., *Update of the global electroweak fit and constraints on two-Higgs-doublet models*, *Eur. Phys. J. C* **78** (2018) 675, arXiv: 1803.01853 [hep-ph].
- [5] M. Sher, *Electroweak Higgs Potentials and Vacuum Stability*, *Phys. Rept.* **179** (1989) 273.
- [6] G. Degrandi et al., *Higgs mass and vacuum stability in the Standard Model at NNLO*, *JHEP* **08** (2012) 098, arXiv: 1205.6497 [hep-ph].
- [7] ATLAS Collaboration, *Measurement of the Higgs boson mass from the $H \rightarrow \gamma\gamma$ and $H \rightarrow ZZ^* \rightarrow 4\ell$ channels in pp collisions at center-of-mass energies of 7 and 8 TeV with the ATLAS detector*, *Phys. Rev. D* **90** (2014) 052004, arXiv: 1406.3827 [hep-ex].
- [8] CMS Collaboration, *Precise determination of the mass of the Higgs boson and tests of compatibility of its couplings with the standard model predictions using proton collisions at 7 and 8 TeV*, *Eur. Phys. J. C* **75** (2015) 212, arXiv: 1412.8662 [hep-ex].
- [9] ATLAS and CMS Collaborations, *Combined Measurement of the Higgs Boson Mass in pp Collisions at $\sqrt{s} = 7$ and 8 TeV with the ATLAS and CMS Experiments*, *Phys. Rev. Lett.* **114** (2015) 191803, arXiv: 1503.07589 [hep-ex].
- [10] ATLAS Collaboration, *Measurement of the Higgs boson mass in the $H \rightarrow ZZ^* \rightarrow 4\ell$ and $H \rightarrow \gamma\gamma$ channels with $\sqrt{s} = 13$ TeV pp collisions using the ATLAS detector*, *Phys. Lett. B* **784** (2018) 345, arXiv: 1806.00242 [hep-ex].
- [11] CMS Collaboration, *A measurement of the Higgs boson mass in the diphoton decay channel*, *Phys. Lett. B* **805** (2020) 135425, arXiv: 2002.06398 [hep-ex].
- [12] ATLAS Collaboration, *Measurement of the Higgs boson mass in the $H \rightarrow ZZ^* \rightarrow 4\ell$ decay channel using 139 fb^{-1} of $\sqrt{s} = 13$ TeV pp collisions recorded by the ATLAS detector at the LHC*, *Phys. Lett. B* **843** (2023) 137880, arXiv: 2207.00320 [hep-ex].
- [13] ATLAS Collaboration, *Electron and photon performance measurements with the ATLAS detector using the 2015–2017 LHC proton–proton collision data*, *JINST* **14** (2019) P12006, arXiv: 1908.00005 [hep-ex].
- [14] ATLAS Collaboration, *Electron and photon energy calibration with the ATLAS detector using LHC Run 2 data*, CERN-EP-2023-128 (2023), arXiv: 2309.05471 [hep-ex].
- [15] ATLAS Collaboration, *The ATLAS Experiment at the CERN Large Hadron Collider*, *JINST* **3** (2008) S08003.

- [16] ATLAS Collaboration, *The ATLAS Collaboration Software and Firmware*, ATL-SOFT-PUB-2021-001, 2021, URL: <https://cds.cern.ch/record/2767187>.
- [17] ATLAS Collaboration, *Performance of electron and photon triggers in ATLAS during LHC Run 2*, *Eur. Phys. J. C* **80** (2020) 47, arXiv: [1909.00761](https://arxiv.org/abs/1909.00761) [hep-ex].
- [18] ATLAS Collaboration, *ATLAS data quality operations and performance for 2015–2018 data-taking*, *JINST* **15** (2020) P04003, arXiv: [1911.04632](https://arxiv.org/abs/1911.04632) [physics.ins-det].
- [19] ATLAS Collaboration, *Luminosity determination in pp collisions at $\sqrt{s} = 13$ TeV using the ATLAS detector at the LHC*, (2022), arXiv: [2212.09379](https://arxiv.org/abs/2212.09379) [hep-ex].
- [20] G. Avoni et al., *The new LUCID-2 detector for luminosity measurement and monitoring in ATLAS*, *JINST* **13** (2018) P07017.
- [21] ATLAS Collaboration, *Measurement of the properties of Higgs boson production at $\sqrt{s} = 13$ TeV in the $H \rightarrow \gamma\gamma$ channel using 139 fb^{-1} of pp collision data with the ATLAS experiment*, *JHEP* **07** (2023) 088, arXiv: [2207.00348](https://arxiv.org/abs/2207.00348) [hep-ex].
- [22] T. Sjöstrand, S. Mrenna and P. Skands, *A brief introduction to PYTHIA 8.1*, *Comput. Phys. Commun.* **178** (2008) 852, arXiv: [0710.3820](https://arxiv.org/abs/0710.3820) [hep-ph].
- [23] S. Alioli, P. Nason, C. Oleari and E. Re, *A general framework for implementing NLO calculations in shower Monte Carlo programs: the POWHEG BOX*, *JHEP* **06** (2010) 043, arXiv: [1002.2581](https://arxiv.org/abs/1002.2581) [hep-ph].
- [24] J. Alwall et al., *The automated computation of tree-level and next-to-leading order differential cross sections, and their matching to parton shower simulations*, *JHEP* **07** (2014) 079, arXiv: [1405.0301](https://arxiv.org/abs/1405.0301) [hep-ph].
- [25] T. Sjöstrand et al., *An introduction to PYTHIA 8.2*, *Comput. Phys. Commun.* **191** (2015) 159, arXiv: [1410.3012](https://arxiv.org/abs/1410.3012) [hep-ph].
- [26] ATLAS Collaboration, *The ATLAS Simulation Infrastructure*, *Eur. Phys. J. C* **70** (2010) 823, arXiv: [1005.4568](https://arxiv.org/abs/1005.4568) [physics.ins-det].
- [27] S. Agostinelli et al., *GEANT4 – a simulation toolkit*, *Nucl. Instrum. Meth. A* **506** (2003) 250.
- [28] J. Bellm et al., *Herwig 7.1 Release Note*, (2017), arXiv: [1705.06919](https://arxiv.org/abs/1705.06919) [hep-ph].
- [29] E. Bothmann et al., *Event generation with Sherpa 2.2*, *SciPost Phys.* **7** (2019) 034, arXiv: [1905.09127](https://arxiv.org/abs/1905.09127) [hep-ph].
- [30] ATLAS Collaboration, *The simulation principle and performance of the ATLAS fast calorimeter simulation FastCaloSim*, ATL-PHYS-PUB-2010-013, 2010, URL: <https://cds.cern.ch/record/1300517>.
- [31] ATLAS Collaboration, *Measurement of Higgs boson production in the diphoton decay channel in pp collisions at center-of-mass energies of 7 and 8 TeV with the ATLAS detector*, *Phys. Rev. D* **90** (2014) 112015, arXiv: [1408.7084](https://arxiv.org/abs/1408.7084) [hep-ex].
- [32] G. Cowan, K. Cranmer, E. Gross and O. Vitells, *Asymptotic formulae for likelihood-based tests of new physics*, *Eur. Phys. J. C* **71** (2011) 1554, arXiv: [1007.1727](https://arxiv.org/abs/1007.1727) [physics.data-an], Erratum: *Eur. Phys. J. C* **73** (2013) 2501.
- [33] ATLAS Collaboration, *Combined search for the Standard Model Higgs boson in pp collisions at $\sqrt{s} = 7$ TeV with the ATLAS detector*, *Phys. Rev. D* **86** (2012) 032003, arXiv: [1207.0319](https://arxiv.org/abs/1207.0319) [hep-ex].

- [34] M. Oreglia, *A Study of the Reactions $\psi' \rightarrow \gamma\gamma\psi$, Appendix D*, (1980), URL: <http://www-public.slac.stanford.edu/sciDoc/docMeta.aspx?slacPubNumber=slac-r-236.html>.
- [35] ATLAS Collaboration, *Electron and photon energy calibration with the ATLAS detector using 2015–2016 LHC proton–proton collision data*, *JINST* **14** (2019) P03017, arXiv: [1812.03848](https://arxiv.org/abs/1812.03848) [[hep-ex](https://arxiv.org/archive/hep)].
- [36] L. Dixon and M. S. Siu, *Resonance-Continuum Interference in the Diphoton Higgs Signal at the LHC*, *Phys. Rev. Lett.* **90** (2003) 252001, arXiv: [hep-ph/0302233](https://arxiv.org/abs/hep-ph/0302233).
- [37] ATLAS Collaboration, *Estimate of the m_H shift due to interference between signal and background processes in the $H \rightarrow \gamma\gamma$ channel, for the $\sqrt{s} = 8$ TeV dataset recorded by ATLAS*, ATL-PHYS-PUB-2016-009, 2016, URL: <https://cds.cern.ch/record/2146386>.
- [38] ATLAS Collaboration, *ATLAS Computing Acknowledgements*, ATL-SOFT-PUB-2023-001, 2023, URL: <https://cds.cern.ch/record/2869272>.
- [39] G. Cowan, K. Cranmer, E. Gross and O. Vitells, *Eur. Phys. J. C* **73** (2013) 2501.

The ATLAS Collaboration

G. Aad ¹⁰², B. Abbott ¹²⁰, K. Abeling ⁵⁵, N.J. Abicht ⁴⁹, S.H. Abidi ²⁹, A. Abouhorma ^{35e}, H. Abramowicz ¹⁵¹, H. Abreu ¹⁵⁰, Y. Abulaiti ¹¹⁷, B.S. Acharya ^{69a,69b,q}, C. Adam Bourdarios ⁴, L. Adamczyk ^{86a}, S.V. Addepalli ²⁶, M.J. Addison ¹⁰¹, J. Adelman ¹¹⁵, A. Adiguzel ^{21c}, T. Adye ¹³⁴, A.A. Affolder ¹³⁶, Y. Afik ³⁶, M.N. Agaras ¹³, J. Agarwala ^{73a,73b}, A. Aggarwal ¹⁰⁰, C. Agheorghiesei ^{27c}, A. Ahmad ³⁶, F. Ahmadov ^{38,ak}, W.S. Ahmed ¹⁰⁴, S. Ahuja ⁹⁵, X. Ai ^{62a}, G. Aielli ^{76a,76b}, A. Aikot ¹⁶³, M. Ait Tamlihat ^{35e}, B. Aitbenchikh ^{35a}, I. Aizenberg ¹⁶⁹, M. Akbiyik ¹⁰⁰, T.P.A. Åkesson ⁹⁸, A.V. Akimov ³⁷, D. Akiyama ¹⁶⁸, N.N. Akolkar ²⁴, K. Al Khoury ⁴¹, G.L. Alberghi ^{23b}, J. Albert ¹⁶⁵, P. Albicocco ⁵³, G.L. Albouy ⁶⁰, S. Alderweireldt ⁵², M. Aleksa ³⁶, I.N. Aleksandrov ³⁸, C. Alexa ^{27b}, T. Alexopoulos ¹⁰, F. Alfonsi ^{23b}, M. Algren ⁵⁶, M. Alhroob ¹²⁰, B. Ali ¹³², H.M.J. Ali ⁹¹, S. Ali ¹⁴⁸, S.W. Alibocus ⁹², M. Aliev ¹⁴⁵, G. Alimonti ^{71a}, W. Alkakhri ⁵⁵, C. Allaire ⁶⁶, B.M.M. Allbrooke ¹⁴⁶, J.F. Allen ⁵², C.A. Allendes Flores ^{137f}, P.P. Allport ²⁰, A. Aloisio ^{72a,72b}, F. Alonso ⁹⁰, C. Alpigiani ¹³⁸, M. Alvarez Estevez ⁹⁹, A. Alvarez Fernandez ¹⁰⁰, M. Alves Cardoso ⁵⁶, M.G. Alviggi ^{72a,72b}, M. Aly ¹⁰¹, Y. Amaral Coutinho ^{83b}, A. Ambler ¹⁰⁴, C. Amelung ³⁶, M. Amerl ¹⁰¹, C.G. Ames ¹⁰⁹, D. Amidei ¹⁰⁶, S.P. Amor Dos Santos ^{130a}, K.R. Amos ¹⁶³, V. Ananiev ¹²⁵, C. Anastopoulos ¹³⁹, T. Andeen ¹¹, J.K. Anders ³⁶, S.Y. Andreev ^{47a,47b}, A. Andreatta ^{71a,71b}, S. Angelidakis ⁹, A. Angerami ^{41,ao}, A.V. Anisenkov ³⁷, A. Annovi ^{74a}, C. Antel ⁵⁶, M.T. Anthony ¹³⁹, E. Antipov ¹⁴⁵, M. Antonelli ⁵³, F. Anulli ^{75a}, M. Aoki ⁸⁴, T. Aoki ¹⁵³, J.A. Aparisi Pozo ¹⁶³, M.A. Aparo ¹⁴⁶, L. Aperio Bella ⁴⁸, C. Appelt ¹⁸, A. Apyan ²⁶, N. Aranzabal ³⁶, S.J. Arbiol Val ⁸⁷, C. Arcangeletti ⁵³, A.T.H. Arce ⁵¹, E. Arena ⁹², J-F. Arguin ¹⁰⁸, S. Argyropoulos ⁵⁴, J.-H. Arling ⁴⁸, O. Arnaez ⁴, H. Arnold ¹¹⁴, G. Artoni ^{75a,75b}, H. Asada ¹¹¹, K. Asai ¹¹⁸, S. Asai ¹⁵³, N.A. Asbah ⁶¹, J. Assahsah ^{35d}, K. Assamagan ²⁹, R. Astalos ^{28a}, S. Atashi ¹⁶⁰, R.J. Atkin ^{33a}, M. Atkinson ¹⁶², H. Atmani ^{35f}, P.A. Atlasiddha ¹⁰⁶, K. Augsten ¹³², S. Auricchio ^{72a,72b}, A.D. Auriol ²⁰, V.A. Austrup ¹⁰¹, G. Avolio ³⁶, K. Axiotis ⁵⁶, G. Azuelos ^{108,av}, D. Babal ^{28b}, H. Bachacou ¹³⁵, K. Bachas ^{152,w}, A. Bachi ³⁴, F. Backman ^{47a,47b}, A. Badea ⁶¹, T.M. Baer ¹⁰⁶, P. Bagnaia ^{75a,75b}, M. Bahmani ¹⁸, A.J. Bailey ¹⁶³, V.R. Bailey ¹⁶², J.T. Baines ¹³⁴, L. Baines ⁹⁴, O.K. Baker ¹⁷², E. Bakos ¹⁵, D. Bakshi Gupta ⁸, V. Balakrishnan ¹²⁰, R. Balasubramanian ¹¹⁴, E.M. Baldin ³⁷, P. Balek ^{86a}, E. Ballabene ^{23b,23a}, F. Balli ¹³⁵, L.M. Baltus ^{63a}, W.K. Balunas ³², J. Balz ¹⁰⁰, E. Banas ⁸⁷, M. Bandieramonte ¹²⁹, A. Bandyopadhyay ²⁴, S. Bansal ²⁴, L. Barak ¹⁵¹, M. Barakat ⁴⁸, E.L. Barberio ¹⁰⁵, D. Barberis ^{57b,57a}, M. Barbero ¹⁰², M.Z. Barel ¹¹⁴, K.N. Barends ^{33a}, T. Barillari ¹¹⁰, M-S. Barisits ³⁶, T. Barklow ¹⁴³, P. Baron ¹²², D.A. Baron Moreno ¹⁰¹, A. Baroncelli ^{62a}, G. Barone ²⁹, A.J. Barr ¹²⁶, J.D. Barr ⁹⁶, L. Barranco Navarro ^{47a,47b}, F. Barreiro ⁹⁹, J. Barreiro Guimarães da Costa ^{14a}, U. Barron ¹⁵¹, M.G. Barros Teixeira ^{130a}, S. Barsov ³⁷, F. Bartels ^{63a}, R. Bartoldus ¹⁴³, A.E. Barton ⁹¹, P. Bartos ^{28a}, A. Basan ^{100,af}, M. Baselga ⁴⁹, A. Bassalat ^{66,b}, M.J. Basso ^{156a}, C.R. Basson ¹⁰¹, R.L. Bates ⁵⁹, S. Batlamous ^{35e}, J.R. Batley ³², B. Batool ¹⁴¹, M. Battaglia ¹³⁶, D. Battulga ¹⁸, M. Bause ^{75a,75b}, M. Bauer ³⁶, P. Bauer ²⁴, L.T. Bazzano Hurrell ³⁰, J.B. Beacham ⁵¹, T. Beau ¹²⁷, J.Y. Beauchamp ⁹⁰, P.H. Beauchemin ¹⁵⁸, F. Becherer ⁵⁴, P. Bechtel ²⁴, H.P. Beck ^{19,u}, K. Becker ¹⁶⁷, A.J. Beddall ⁸², V.A. Bednyakov ³⁸, C.P. Bee ¹⁴⁵, L.J. Beemster ¹⁵, T.A. Beermann ³⁶, M. Begalli ^{83d}, M. Beger ²⁹, A. Behera ¹⁴⁵, J.K. Behr ⁴⁸, J.F. Beirer ⁵⁵, F. Beisiegel ²⁴, M. Belfkir ¹⁵⁹, G. Bella ¹⁵¹, L. Bellagamba ^{23b}, A. Bellerive ³⁴, P. Bellos ²⁰, K. Beloborodov ³⁷, D. Benckroun ^{35a}, F. Bendebba ^{35a}, Y. Benhammou ¹⁵¹, M. Benoit ²⁹, J.R. Bensinger ²⁶,

S. Bentvelsen ¹¹⁴, L. Beresford ⁴⁸, M. Beretta ⁵³, E. Bergeaas Kuutmann ¹⁶¹, N. Berger ⁴,
 B. Bergmann ¹³², J. Beringer ^{17a}, G. Bernardi ⁵, C. Bernius ¹⁴³, F.U. Bernlochner ²⁴,
 F. Bernon ^{36,102}, A. Berrocal Guardia ¹³, T. Berry ⁹⁵, P. Berta ¹³³, A. Berthold ⁵⁰,
 I.A. Bertram ⁹¹, S. Bethke ¹¹⁰, A. Betti ^{75a,75b}, A.J. Bevan ⁹⁴, N.K. Bhalla ⁵⁴, M. Bhamjee ^{33c},
 S. Bhatta ¹⁴⁵, D.S. Bhattacharya ¹⁶⁶, P. Bhattarai ¹⁴³, V.S. Bhopatkar ¹²¹, R. Bi ^{29,ay},
 R.M. Bianchi ¹²⁹, G. Bianco ^{23b,23a}, O. Biebel ¹⁰⁹, R. Bielski ¹²³, M. Biglietti ^{77a}, M. Bindi ⁵⁵,
 A. Bingul ^{21b}, C. Bini ^{75a,75b}, A. Biondini ⁹², C.J. Birch-sykes ¹⁰¹, G.A. Bird ^{20,134},
 M. Birman ¹⁶⁹, M. Biros ¹³³, S. Biryukov ¹⁴⁶, T. Bisanz ⁴⁹, E. Bisceglie ^{43b,43a}, J.P. Biswal ¹³⁴,
 D. Biswas ¹⁴¹, A. Bitadze ¹⁰¹, K. Bjørke ¹²⁵, I. Bloch ⁴⁸, C. Blocker ²⁶, A. Blue ⁵⁹,
 U. Blumenschein ⁹⁴, J. Blumenthal ¹⁰⁰, G.J. Bobbink ¹¹⁴, V.S. Bobrovnikov ³⁷, M. Boehler ⁵⁴,
 B. Boehm ¹⁶⁶, D. Bogavac ³⁶, A.G. Bogdanchikov ³⁷, C. Bohm ^{47a}, V. Boisvert ⁹⁵, P. Bokan ⁴⁸,
 T. Bold ^{86a}, M. Bomben ⁵, M. Bona ⁹⁴, M. Boonekamp ¹³⁵, C.D. Booth ⁹⁵, A.G. Borbély ^{59,as},
 I.S. Bordulev ³⁷, H.M. Borecka-Bielska ¹⁰⁸, G. Borissov ⁹¹, D. Bortoletto ¹²⁶, D. Boscherini ^{23b},
 M. Bosman ¹³, J.D. Bossio Sola ³⁶, K. Bouaouda ^{35a}, N. Bouchhar ¹⁶³, J. Boudreau ¹²⁹,
 E.V. Bouhova-Thacker ⁹¹, D. Boumediene ⁴⁰, R. Bouquet ¹⁶⁵, A. Boveia ¹¹⁹, J. Boyd ³⁶,
 D. Boye ²⁹, I.R. Boyko ³⁸, J. Bracik ²⁰, N. Brahimi ^{62d}, G. Brandt ¹⁷¹, O. Brandt ³²,
 F. Braren ⁴⁸, B. Brau ¹⁰³, J.E. Brau ¹²³, R. Brenner ¹⁶⁹, L. Brenner ¹¹⁴, R. Brenner ¹⁶¹,
 S. Bressler ¹⁶⁹, D. Britton ⁵⁹, D. Britzger ¹¹⁰, I. Brock ²⁴, G. Brooijmans ⁴¹, W.K. Brooks ^{137f},
 E. Brost ²⁹, L.M. Brown ^{165,n}, L.E. Bruce ⁶¹, T.L. Bruckler ¹²⁶, P.A. Bruckman de Renstrom ⁸⁷,
 B. Brüers ⁴⁸, A. Bruni ^{23b}, G. Bruni ^{23b}, M. Bruschi ^{23b}, N. Bruscinò ^{75a,75b}, T. Buanes ¹⁶,
 Q. Buat ¹³⁸, D. Buchin ¹¹⁰, A.G. Buckley ⁵⁹, O. Bulekov ³⁷, B.A. Bullard ¹⁴³, S. Burdin ⁹²,
 C.D. Burgard ⁴⁹, A.M. Burger ⁴⁰, B. Burghgrave ⁸, O. Burlayenko ⁵⁴, J.T.P. Burr ³²,
 C.D. Burton ¹¹, J.C. Burzynski ¹⁴², E.L. Busch ⁴¹, V. Büscher ¹⁰⁰, P.J. Bussey ⁵⁹,
 J.M. Butler ²⁵, C.M. Buttar ⁵⁹, J.M. Butterworth ⁹⁶, W. Buttinger ¹³⁴, C.J. Buxo Vazquez ¹⁰⁷,
 A.R. Buzykaev ³⁷, S. Cabrera Urbán ¹⁶³, L. Cadamuro ⁶⁶, D. Caforio ⁵⁸, H. Cai ¹²⁹,
 Y. Cai ^{14a,14e}, Y. Cai ^{14c}, V.M.M. Cairo ³⁶, O. Cakir ^{3a}, N. Calace ³⁶, P. Calafiura ^{17a},
 G. Calderini ¹²⁷, P. Calfayan ⁶⁸, G. Callea ⁵⁹, L.P. Caloba ^{83b}, D. Calvet ⁴⁰, S. Calvet ⁴⁰,
 T.P. Calvet ¹⁰², M. Calvetti ^{74a,74b}, R. Camacho Toro ¹²⁷, S. Camarda ³⁶, D. Camarero Munoz ²⁶,
 P. Camarri ^{76a,76b}, M.T. Camerlingo ^{72a,72b}, D. Cameron ^{36,h}, C. Camincher ¹⁶⁵,
 M. Campanelli ⁹⁶, A. Camplani ⁴², V. Canale ^{72a,72b}, A. Canesse ¹⁰⁴, J. Cantero ¹⁶³, Y. Cao ¹⁶²,
 F. Capocasa ²⁶, M. Capua ^{43b,43a}, A. Carbone ^{71a,71b}, R. Cardarelli ^{76a}, J.C.J. Cardenas ⁸,
 F. Cardillo ¹⁶³, G. Carducci ^{43b,43a}, T. Carli ³⁶, G. Carlino ^{72a}, J.I. Carlotto ¹³, B.T. Carlson ^{129,x},
 E.M. Carlson ^{165,156a}, L. Carminati ^{71a,71b}, A. Carnelli ¹³⁵, M. Carnesale ^{75a,75b}, S. Caron ¹¹³,
 E. Carquin ^{137f}, S. Carrá ^{71a,71b}, G. Carratta ^{23b,23a}, F. Carri Argos ^{33g}, J.W.S. Carter ¹⁵⁵,
 T.M. Carter ⁵², M.P. Casado ^{13,k}, M. Caspar ⁴⁸, F.L. Castillo ⁴, L. Castillo Garcia ¹³,
 V. Castillo Gimenez ¹⁶³, N.F. Castro ^{130a,130e}, A. Catinaccio ³⁶, J.R. Catmore ¹²⁵, V. Cavaliere ²⁹,
 N. Cavalli ^{23b,23a}, V. Cavalinì ^{74a,74b}, Y.C. Cekmecelioglu ⁴⁸, E. Celebi ^{21a}, F. Celli ¹²⁶,
 M.S. Centonze ^{70a,70b}, V. Cepaitis ⁵⁶, K. Cerny ¹²², A.S. Cerqueira ^{83a}, A. Cerri ¹⁴⁶,
 L. Cerrito ^{76a,76b}, F. Cerutti ^{17a}, B. Cervato ¹⁴¹, A. Cervelli ^{23b}, G. Cesarini ⁵³, S.A. Cetin ⁸²,
 Z. Chadi ^{35a}, D. Chakraborty ¹¹⁵, J. Chan ¹⁷⁰, W.Y. Chan ¹⁵³, J.D. Chapman ³², E. Chapon ¹³⁵,
 B. Chargeishvili ^{149b}, D.G. Charlton ²⁰, T.P. Charman ⁹⁴, M. Chatterjee ¹⁹, C. Chauhan ¹³³,
 S. Chekanov ⁶, S.V. Chekulaev ^{156a}, G.A. Chelkov ^{38,a}, A. Chen ¹⁰⁶, B. Chen ¹⁵¹, B. Chen ¹⁶⁵,
 H. Chen ^{14c}, H. Chen ²⁹, J. Chen ^{62c}, J. Chen ¹⁴², M. Chen ¹²⁶, S. Chen ¹⁵³, S.J. Chen ^{14c},
 X. Chen ^{62c,135}, X. Chen ^{14b,au}, Y. Chen ^{62a}, C.L. Cheng ¹⁷⁰, H.C. Cheng ^{64a}, S. Cheong ¹⁴³,
 A. Cheplakov ³⁸, E. Cheremushkina ⁴⁸, E. Cherepanova ¹¹⁴, R. Cherkaoui El Moursli ^{35e},
 E. Cheu ⁷, K. Cheung ⁶⁵, L. Chevalier ¹³⁵, V. Chiarella ⁵³, G. Chiarelli ^{74a}, N. Chiedde ¹⁰²,
 G. Chiodini ^{70a}, A.S. Chisholm ²⁰, A. Chitan ^{27b}, M. Chitishvili ¹⁶³, M.V. Chizhov ³⁸,

K. Choi ¹¹, A.R. Chomont ^{75a,75b}, Y. Chou ¹⁰³, E.Y.S. Chow ¹¹³, T. Chowdhury ^{33g}, K.L. Chu ¹⁶⁹,
 M.C. Chu ^{64a}, X. Chu ^{14a,14e}, J. Chudoba ¹³¹, J.J. Chwastowski ⁸⁷, D. Cieri ¹¹⁰, K.M. Ciesla ^{86a},
 V. Cindro ⁹³, A. Ciocio ^{17a}, F. Cirotto ^{72a,72b}, Z.H. Citron ^{169,o}, M. Citterio ^{71a},
 D.A. Ciubotaru ^{27b}, B.M. Ciungu ¹⁵⁵, A. Clark ⁵⁶, P.J. Clark ⁵², C. Clarry ¹⁵⁵,
 J.M. Clavijo Columbie ⁴⁸, S.E. Clawson ⁴⁸, C. Clement ^{47a,47b}, J. Clercx ⁴⁸, L. Clissa ^{23b,23a},
 Y. Coadou ¹⁰², M. Cobal ^{69a,69c}, A. Coccaro ^{57b}, R.F. Coelho Barrue ^{130a},
 R. Coelho Lopes De Sa ¹⁰³, S. Coelli ^{71a}, H. Cohen ¹⁵¹, A.E.C. Coimbra ^{71a,71b}, B. Cole ⁴¹,
 J. Collot ⁶⁰, P. Conde Muño ^{130a,130g}, M.P. Connell ^{33c}, S.H. Connell ^{33c}, I.A. Connelly ⁵⁹,
 E.I. Conroy ¹²⁶, F. Conventi ^{72a,aw}, H.G. Cooke ²⁰, A.M. Cooper-Sarkar ¹²⁶,
 A. Cordeiro Oudot Choi ¹²⁷, L.D. Corpe ⁴⁰, M. Corradi ^{75a,75b}, F. Corriveau ^{104,ai},
 A. Cortes-Gonzalez ¹⁸, M.J. Costa ¹⁶³, F. Costanza ⁴, D. Costanzo ¹³⁹, B.M. Cote ¹¹⁹,
 G. Cowan ⁹⁵, K. Cranmer ¹⁷⁰, D. Cremonini ^{23b,23a}, S. Crépe-Renaudin ⁶⁰, F. Crescioli ¹²⁷,
 M. Cristinziani ¹⁴¹, M. Cristoforetti ^{78a,78b}, V. Croft ¹¹⁴, J.E. Crosby ¹²¹, G. Crosetti ^{43b,43a},
 A. Cueto ⁹⁹, T. Cuhadar Donszelmann ¹⁶⁰, H. Cui ^{14a,14e}, Z. Cui ⁷, W.R. Cunningham ⁵⁹,
 F. Curcio ^{43b,43a}, P. Czodrowski ³⁶, M.M. Czurylo ^{63b}, M.J. Da Cunha Sargedas De Sousa ^{57b,57a},
 J.V. Da Fonseca Pinto ^{83b}, C. Da Via ¹⁰¹, W. Dabrowski ^{86a}, T. Dado ⁴⁹, S. Dahbi ^{33g},
 T. Dai ¹⁰⁶, D. Dal Santo ¹⁹, C. Dallapiccola ¹⁰³, M. Dam ⁴², G. D'amen ²⁹, V. D'Amico ¹⁰⁹,
 J. Damp ¹⁰⁰, J.R. Dandoy ¹²⁸, M.F. Daneri ³⁰, M. Danninger ¹⁴², V. Dao ³⁶, G. Darbo ^{57b},
 S. Darmora ⁶, S.J. Das ^{29,ay}, S. D'Auria ^{71a,71b}, C. David ^{156b}, T. Davidek ¹³³,
 B. Davis-Purcell ³⁴, I. Dawson ⁹⁴, H.A. Day-hall ¹³², K. De ⁸, R. De Asmundis ^{72a},
 N. De Biase ⁴⁸, S. De Castro ^{23b,23a}, N. De Groot ¹¹³, P. de Jong ¹¹⁴, H. De la Torre ¹¹⁵,
 A. De Maria ^{14c}, A. De Salvo ^{75a}, U. De Sanctis ^{76a,76b}, A. De Santo ¹⁴⁶,
 J.B. De Vivie De Regie ⁶⁰, D.V. Dedovich ³⁸, J. Degens ¹¹⁴, A.M. Deiana ⁴⁴, F. Del Corso ^{23b,23a},
 J. Del Peso ⁹⁹, F. Del Rio ^{63a}, F. Deliot ¹³⁵, C.M. Delitzsch ⁴⁹, M. Della Pietra ^{72a,72b},
 D. Della Volpe ⁵⁶, A. Dell'Acqua ³⁶, L. Dell'Asta ^{71a,71b}, M. Delmastro ⁴, P.A. Delsart ⁶⁰,
 S. Demers ¹⁷², M. Demichev ³⁸, S.P. Denisov ³⁷, L. D'Eramo ⁴⁰, D. Derendarz ⁸⁷, F. Derue ¹²⁷,
 P. Dervan ⁹², K. Desch ²⁴, C. Deutsch ²⁴, F.A. Di Bello ^{57b,57a}, A. Di Ciaccio ^{76a,76b},
 L. Di Ciaccio ⁴, A. Di Domenico ^{75a,75b}, C. Di Donato ^{72a,72b}, A. Di Girolamo ³⁶,
 G. Di Gregorio ³⁶, A. Di Luca ^{78a,78b}, B. Di Micco ^{77a,77b}, R. Di Nardo ^{77a,77b}, C. Diaconu ¹⁰²,
 M. Diamantopoulou ³⁴, F.A. Dias ¹¹⁴, T. Dias Do Vale ¹⁴², M.A. Diaz ^{137a,137b},
 F.G. Diaz Capriles ²⁴, M. Didenko ¹⁶³, E.B. Diehl ¹⁰⁶, L. Diehl ⁵⁴, S. Díez Cornell ⁴⁸,
 C. Diez Pardos ¹⁴¹, C. Dimitriadi ^{161,24,161}, A. Dimitrievska ^{17a}, J. Dingfelder ²⁴, I-M. Dinu ^{27b},
 S.J. Dittmeier ^{63b}, F. Dittus ³⁶, F. Djama ¹⁰², T. Djobava ^{149b}, J.I. Djuvsland ¹⁶,
 C. Doglioni ^{101,98}, A. Dohnalova ^{28a}, J. Dolejsi ¹³³, Z. Dolezal ¹³³, K.M. Dona ³⁹,
 M. Donadelli ^{83c}, B. Dong ¹⁰⁷, J. Donini ⁴⁰, A. D'Onofrio ^{77a,77b}, M. D'Onofrio ⁹²,
 J. Dopke ¹³⁴, A. Doria ^{72a}, N. Dos Santos Fernandes ^{130a}, P. Dougan ¹⁰¹, M.T. Dova ⁹⁰,
 A.T. Doyle ⁵⁹, M.A. Dragnet ¹²⁶, E. Dreyer ¹⁶⁹, I. Drivas-koulouris ¹⁰, M. Drnevich ¹¹⁷,
 A.S. Drobac ¹⁵⁸, M. Drozdova ⁵⁶, D. Du ^{62a}, T.A. du Pree ¹¹⁴, F. Dubinin ³⁷, M. Dubovsky ^{28a},
 E. Duchovni ¹⁶⁹, G. Duckeck ¹⁰⁹, O.A. Ducu ^{27b}, D. Duda ⁵², A. Dudarev ³⁶, E.R. Duden ²⁶,
 M. D'uffizi ¹⁰¹, L. Duflot ⁶⁶, M. Dührssen ³⁶, C. Dülsen ¹⁷¹, A.E. Dumitriu ^{27b}, M. Dunford ^{63a},
 S. Dungs ⁴⁹, K. Dunne ^{47a,47b}, A. Duperrin ¹⁰², H. Duran Yildiz ^{3a}, M. Düren ⁵⁸,
 A. Durglishvili ^{149b}, B.L. Dwyer ¹¹⁵, G.I. Dyckes ^{17a}, M. Dyndal ^{86a}, B.S. Dziedzic ⁸⁷,
 Z.O. Earnshaw ¹⁴⁶, G.H. Eberwein ¹²⁶, B. Eckerova ^{28a}, S. Eggebrecht ⁵⁵,
 E. Egidio Purcino De Souza ¹²⁷, L.F. Ehrke ⁵⁶, G. Eigen ¹⁶, K. Einsweiler ^{17a}, T. Ekelof ¹⁶¹,
 P.A. Ekman ⁹⁸, S. El Farkh ^{35b}, Y. El Ghazali ^{35b}, H. El Jarrari ^{35e,148}, A. El Moussaouy ^{108,ab},
 V. Ellajosyula ¹⁶¹, M. Ellert ¹⁶¹, F. Ellinghaus ¹⁷¹, N. Ellis ³⁶, J. Elmsheuser ²⁹, M. Elsing ³⁶,
 D. Emelianov ¹³⁴, Y. Enari ¹⁵³, I. Ene ^{17a}, S. Epari ¹³, J. Erdmann ⁴⁹, P.A. Erland ⁸⁷,

M. Errenst ¹⁷¹, M. Escalier ⁶⁶, C. Escobar ¹⁶³, E. Etzion ¹⁵¹, G. Evans ^{130a}, H. Evans ⁶⁸,
 L.S. Evans ⁹⁵, M.O. Evans ¹⁴⁶, A. Ezhilov ³⁷, S. Ezzarqtouni ^{35a}, F. Fabbri ⁵⁹, L. Fabbri ^{23b,23a},
 G. Facini ⁹⁶, V. Fadeyev ¹³⁶, R.M. Fakhrutdinov ³⁷, S. Falciano ^{75a}, L.F. Falda Ulhoa Coelho ³⁶,
 P.J. Falke ²⁴, J. Faltova ¹³³, C. Fan ¹⁶², Y. Fan ^{14a}, Y. Fang ^{14a,14e}, M. Fanti ^{71a,71b},
 M. Faraj ^{69a,69b}, Z. Farazpay ⁹⁷, A. Farbin ⁸, A. Farilla ^{77a}, T. Farooque ¹⁰⁷, S.M. Farrington ⁵²,
 F. Fassi ^{35e}, D. Fassouliotis ⁹, M. Faucci Giannelli ^{76a,76b}, W.J. Fawcett ³², L. Fayard ⁶⁶,
 P. Federic ¹³³, P. Federicova ¹³¹, O.L. Fedin ^{37,a}, G. Fedotov ³⁷, M. Feickert ¹⁷⁰,
 L. Feligioni ¹⁰², D.E. Fellers ¹²³, C. Feng ^{62b}, M. Feng ^{14b}, Z. Feng ¹¹⁴, M.J. Fenton ¹⁶⁰,
 A.B. Fenyuk ³⁷, L. Ferencz ⁴⁸, R.A.M. Ferguson ⁹¹, S.I. Fernandez Luengo ^{137f},
 P. Fernandez Martinez ¹³, M.J.V. Fernoux ¹⁰², J. Ferrando ⁴⁸, A. Ferrari ¹⁶¹, P. Ferrari ^{114,113},
 R. Ferrari ^{73a}, D. Ferrere ⁵⁶, C. Ferretti ¹⁰⁶, F. Fiedler ¹⁰⁰, P. Fiedler ¹³², A. Filipčič ⁹³,
 E.K. Filmer ¹, F. Filthaut ¹¹³, M.C.N. Fiolhais ^{130a,130c,d}, L. Fiorini ¹⁶³, W.C. Fisher ¹⁰⁷,
 T. Fitschen ¹⁰¹, P.M. Fitzhugh ¹³⁵, I. Fleck ¹⁴¹, P. Fleischmann ¹⁰⁶, T. Flick ¹⁷¹, M. Flores ^{33d,ap},
 L.R. Flores Castillo ^{64a}, L. Flores Sanz De Acedo ³⁶, F.M. Follega ^{78a,78b}, N. Fomin ¹⁶,
 J.H. Foo ¹⁵⁵, B.C. Forland ⁶⁸, A. Formica ¹³⁵, A.C. Forti ¹⁰¹, E. Fortin ³⁶, A.W. Fortman ⁶¹,
 M.G. Foti ^{17a}, L. Fountas ^{9,1}, D. Fournier ⁶⁶, H. Fox ⁹¹, P. Francavilla ^{74a,74b}, S. Francescato ⁶¹,
 S. Franchellucci ⁵⁶, M. Franchini ^{23b,23a}, S. Franchino ^{63a}, D. Francis ³⁶, L. Franco ¹¹³,
 V. Franco Lima ³⁶, L. Franconi ⁴⁸, M. Franklin ⁶¹, G. Frattari ²⁶, A.C. Freegard ⁹⁴,
 W.S. Freund ^{83b}, Y.Y. Frid ¹⁵¹, J. Friend ⁵⁹, N. Fritzsche ⁵⁰, A. Froch ⁵⁴, D. Froidevaux ³⁶,
 J.A. Frost ¹²⁶, Y. Fu ^{62a}, S. Fuenzalida Garrido ^{137f}, M. Fujimoto ¹⁰², E. Fullana Torregrosa ^{163,*},
 K.Y. Fung ^{64a}, E. Furtado De Simas Filho ^{83b}, M. Furukawa ¹⁵³, J. Fuster ¹⁶³, A. Gabrielli ^{23b,23a},
 A. Gabrielli ¹⁵⁵, P. Gadow ³⁶, G. Gagliardi ^{57b,57a}, L.G. Gagnon ^{17a}, E.J. Gallas ¹²⁶,
 B.J. Gallop ¹³⁴, K.K. Gan ¹¹⁹, S. Ganguly ¹⁵³, Y. Gao ⁵², F.M. Garay Walls ^{137a,137b},
 B. Garcia ^{29,ay}, C. García ¹⁶³, A. Garcia Alonso ¹¹⁴, A.G. Garcia Caffaro ¹⁷²,
 J.E. García Navarro ¹⁶³, M. Garcia-Sciveres ^{17a}, G.L. Gardner ¹²⁸, R.W. Gardner ³⁹,
 N. Garelli ¹⁵⁸, D. Garg ⁸⁰, R.B. Garg ^{143,t}, J.M. Gargan ⁵², C.A. Garner ¹⁵⁵, C.M. Garvey ^{33a},
 P. Gaspar ^{83b}, V.K. Gassmann ¹⁵⁸, G. Gaudio ^{73a}, V. Gautam ¹³, P. Gauzzi ^{75a,75b}, I.L. Gavrilenko ³⁷,
 A. Gavriluk ³⁷, C. Gay ¹⁶⁴, G. Gaycken ⁴⁸, E.N. Gazis ¹⁰, A.A. Geanta ^{27b}, C.M. Gee ¹³⁶,
 A. Gekow ¹¹⁹, C. Gemme ^{57b}, M.H. Genest ⁶⁰, S. Gentile ^{75a,75b}, A.D. Gentry ¹¹², S. George ⁹⁵,
 W.F. George ²⁰, T. Geralis ⁴⁶, P. Gessinger-Befurt ³⁶, M.E. Geyik ¹⁷¹, M. Ghani ¹⁶⁷,
 M. Ghneimat ¹⁴¹, K. Ghorbanian ⁹⁴, A. Ghosal ¹⁴¹, A. Ghosh ¹⁶⁰, A. Ghosh ⁷, B. Giacobbe ^{23b},
 S. Giagu ^{75a,75b}, T. Giani ¹¹⁴, P. Giannetti ^{74a}, A. Giannini ^{62a}, S.M. Gibson ⁹⁵, M. Gignac ¹³⁶,
 D.T. Gil ^{86b}, A.K. Gilbert ^{86a}, B.J. Gilbert ⁴¹, D. Gillberg ³⁴, G. Gilles ¹¹⁴, N.E.K. Gillwald ⁴⁸,
 L. Ginabat ¹²⁷, D.M. Gingrich ^{2,av}, M.P. Giordani ^{69a,69c}, P.F. Giraud ¹³⁵, G. Giugliarelli ^{69a,69c},
 D. Giugni ^{71a}, F. Giuli ³⁶, I. Gkialas ^{9,1}, L.K. Gladilin ³⁷, C. Glasman ⁹⁹, G.R. Gledhill ¹²³,
 G. Glemža ⁴⁸, M. Glisic ¹²³, I. Gnesi ^{43b,g}, Y. Go ^{29,ay}, M. Goblirsch-Kolb ³⁶, B. Gocke ⁴⁹,
 D. Godin ¹⁰⁸, B. Gokturk ^{21a}, S. Goldfarb ¹⁰⁵, T. Golling ⁵⁶, M.G.D. Gololo ^{33g}, D. Golubkov ³⁷,
 J.P. Gombas ¹⁰⁷, A. Gomes ^{130a,130b}, G. Gomes Da Silva ¹⁴¹, A.J. Gomez Delegido ¹⁶³,
 R. Gonçalves ^{130a,130c}, G. Gonella ¹²³, L. Gonella ²⁰, A. Gongadze ^{149c}, F. Gonnella ²⁰,
 J.L. Gonski ⁴¹, R.Y. González Andana ⁵², S. González de la Hoz ¹⁶³, S. Gonzalez Fernandez ¹³,
 R. Gonzalez Lopez ⁹², C. Gonzalez Renteria ^{17a}, M.V. Gonzalez Rodrigues ⁴⁸,
 R. Gonzalez Suarez ¹⁶¹, S. Gonzalez-Sevilla ⁵⁶, G.R. Gonzalvo Rodriguez ¹⁶³, L. Goossens ³⁶,
 B. Gorini ³⁶, E. Gorini ^{70a,70b}, A. Gorišek ⁹³, T.C. Gosart ¹²⁸, A.T. Goshaw ⁵¹, M.I. Gostkin ³⁸,
 S. Goswami ¹²¹, C.A. Gottardo ³⁶, S.A. Gotz ¹⁰⁹, M. Gouighri ^{35b}, V. Goumarre ⁴⁸,
 A.G. Goussiou ¹³⁸, N. Govender ^{33c}, I. Grabowska-Bold ^{86a}, K. Graham ³⁴, E. Gramstad ¹²⁵,
 S. Grancagnolo ^{70a,70b}, M. Grandi ¹⁴⁶, C.M. Grant ^{1,135}, P.M. Gravila ^{27f}, F.G. Gravili ^{70a,70b},
 H.M. Gray ^{17a}, M. Greco ^{70a,70b}, C. Grefe ²⁴, I.M. Gregor ⁴⁸, P. Grenier ¹⁴³, S.G. Grewe ¹¹⁰,

C. Grieco ¹³, A.A. Grillo ¹³⁶, K. Grimm ³¹, S. Grinstein ^{13,ad}, J.-F. Grivaz ⁶⁶, E. Gross ¹⁶⁹,
 J. Grosse-Knetter ⁵⁵, C. Grud ¹⁰⁶, J.C. Grundy ¹²⁶, L. Guan ¹⁰⁶, W. Guan ²⁹, C. Gubbels ¹⁶⁴,
 J.G.R. Guerrero Rojas ¹⁶³, G. Guerrieri ^{69a,69c}, F. Guescini ¹¹⁰, R. Gugel ¹⁰⁰, J.A.M. Guhit ¹⁰⁶,
 A. Guida ¹⁸, T. Guillemain ⁴, E. Guilloton ^{167,134}, S. Guindon ³⁶, F. Guo ^{14a,14e}, J. Guo ^{62c},
 L. Guo ⁴⁸, Y. Guo ¹⁰⁶, R. Gupta ⁴⁸, R. Gupta ¹²⁹, S. Gurbuz ²⁴, S.S. Gurdasani ⁵⁴,
 G. Gustavino ³⁶, M. Guth ⁵⁶, P. Gutierrez ¹²⁰, L.F. Gutierrez Zagazeta ¹²⁸, M. Gutsche ⁵⁰,
 C. Gutschow ⁹⁶, C. Gwenlan ¹²⁶, C.B. Gwilliam ⁹², E.S. Haaland ¹²⁵, A. Haas ¹¹⁷,
 M. Habedank ⁴⁸, C. Haber ^{17a}, H.K. Hadavand ⁸, A. Hadeef ¹⁰⁰, S. Hadzic ¹¹⁰, A.I. Hagan ⁹¹,
 J.J. Hahn ¹⁴¹, E.H. Haines ⁹⁶, M. Haleem ¹⁶⁶, J. Haley ¹²¹, J.J. Hall ¹³⁹, G.D. Hallelwell ¹⁰²,
 L. Halser ¹⁹, K. Hamano ¹⁶⁵, M. Hamer ²⁴, G.N. Hamity ⁵², E.J. Hampshire ⁹⁵, J. Han ^{62b},
 K. Han ^{62a}, L. Han ^{14c}, L. Han ^{62a}, S. Han ^{17a}, Y.F. Han ¹⁵⁵, K. Hanagaki ⁸⁴, M. Hance ¹³⁶,
 D.A. Hangal ^{41,ao}, H. Hanif ¹⁴², M.D. Hank ¹²⁸, R. Hankache ¹⁰¹, J.B. Hansen ⁴²,
 J.D. Hansen ⁴², P.H. Hansen ⁴², K. Hara ¹⁵⁷, D. Harada ⁵⁶, T. Harenberg ¹⁷¹, S. Harkusha ³⁷,
 M.L. Harris ¹⁰³, Y.T. Harris ¹²⁶, J. Harrison ¹³, N.M. Harrison ¹¹⁹, P.F. Harrison ¹⁶⁷,
 N.M. Hartman ¹¹⁰, N.M. Hartmann ¹⁰⁹, Y. Hasegawa ¹⁴⁰, R. Hauser ¹⁰⁷, C.M. Hawkes ²⁰,
 R.J. Hawkings ³⁶, Y. Hayashi ¹⁵³, S. Hayashida ¹¹¹, D. Hayden ¹⁰⁷, C. Hayes ¹⁰⁶,
 R.L. Hayes ¹¹⁴, C.P. Hays ¹²⁶, J.M. Hays ⁹⁴, H.S. Hayward ⁹², F. He ^{62a}, M. He ^{14a,14e},
 Y. He ¹⁵⁴, Y. He ⁴⁸, N.B. Heatley ⁹⁴, V. Hedberg ⁹⁸, A.L. Heggelund ¹²⁵, N.D. Hehir ⁹⁴,
 C. Heidegger ⁵⁴, K.K. Heidegger ⁵⁴, W.D. Heidorn ⁸¹, J. Heilman ³⁴, S. Heim ⁴⁸, T. Heim ^{17a},
 J.G. Heinlein ¹²⁸, J.J. Heinrich ¹²³, L. Heinrich ^{110,at}, J. Hejbal ¹³¹, L. Helary ⁴⁸, A. Held ¹⁷⁰,
 S. Hellesund ¹⁶, C.M. Helling ¹⁶⁴, S. Hellman ^{47a,47b}, R.C.W. Henderson ⁹¹, L. Henkelmann ³²,
 A.M. Henriques Correia ³⁶, H. Herde ⁹⁸, Y. Hernández Jiménez ¹⁴⁵, L.M. Herrmann ²⁴,
 T. Herrmann ⁵⁰, G. Herten ⁵⁴, R. Hertenberger ¹⁰⁹, L. Hervas ³⁶, M.E. Hesping ¹⁰⁰,
 N.P. Hessey ^{156a}, H. Hibi ⁸⁵, E. Hill ¹⁵⁵, S.J. Hillier ²⁰, J.R. Hinds ¹⁰⁷, F. Hinterkeuser ²⁴,
 M. Hirose ¹²⁴, S. Hirose ¹⁵⁷, D. Hirschbuehl ¹⁷¹, T.G. Hitchings ¹⁰¹, B. Hiti ⁹³, J. Hobbs ¹⁴⁵,
 R. Hobincu ^{27e}, N. Hod ¹⁶⁹, M.C. Hodgkinson ¹³⁹, B.H. Hodgkinson ³², A. Hoecker ³⁶,
 D.D. Hofer ¹⁰⁶, J. Hofer ⁴⁸, T. Holm ²⁴, M. Holzbock ¹¹⁰, L.B.A.H. Hommels ³²,
 B.P. Honan ¹⁰¹, J. Hong ^{62c}, T.M. Hong ¹²⁹, B.H. Hooberman ¹⁶², W.H. Hopkins ⁶, Y. Horii ¹¹¹,
 S. Hou ¹⁴⁸, A.S. Howard ⁹³, J. Howarth ⁵⁹, J. Hoya ⁶, M. Hrabovsky ¹²², A. Hrynevich ⁴⁸,
 T. Hryn'ova ⁴, P.J. Hsu ⁶⁵, S.-C. Hsu ¹³⁸, Q. Hu ^{62a}, Y.F. Hu ^{14a,14e}, S. Huang ^{64b},
 X. Huang ^{14c}, X. Huang ^{14a,14e}, Y. Huang ^{139,m}, Y. Huang ^{14a}, Z. Huang ¹⁰¹, Z. Hubacek ¹³²,
 M. Huebner ²⁴, F. Huegging ²⁴, T.B. Huffman ¹²⁶, C.A. Hugli ⁴⁸, M. Huhtinen ³⁶,
 S.K. Huiberts ¹⁶, R. Hulsken ¹⁰⁴, N. Huseynov ¹², J. Huston ¹⁰⁷, J. Huth ⁶¹, R. Hyneman ¹⁴³,
 G. Iacobucci ⁵⁶, G. Iakovidis ²⁹, I. Ibragimov ¹⁴¹, L. Iconomidou-Fayard ⁶⁶, P. Iengo ^{72a,72b},
 R. Iguchi ¹⁵³, T. Iizawa ^{126,r}, Y. Ikegami ⁸⁴, N. Ilic ¹⁵⁵, H. Imam ^{35a}, M. Ince Lezki ⁵⁶,
 T. Ingebretsen Carlson ^{47a,47b}, G. Introzzi ^{73a,73b}, M. Iodice ^{77a}, V. Ippolito ^{75a,75b}, R.K. Irwin ⁹²,
 M. Ishino ¹⁵³, W. Islam ¹⁷⁰, C. Issever ^{18,48}, S. Istin ^{21a,ba}, H. Ito ¹⁶⁸, J.M. Iturbe Ponce ^{64a},
 R. Iuppa ^{78a,78b}, A. Ivina ¹⁶⁹, J.M. Izen ⁴⁵, V. Izzo ^{72a}, P. Jacka ^{131,132}, P. Jackson ¹,
 R.M. Jacobs ⁴⁸, B.P. Jaeger ¹⁴², C.S. Jagfeld ¹⁰⁹, G. Jain ^{156a}, P. Jain ⁵⁴, K. Jakobs ⁵⁴,
 T. Jakoubek ¹⁶⁹, J. Jamieson ⁵⁹, K.W. Janas ^{86a}, M. Javurkova ¹⁰³, F. Jeanneau ¹³⁵,
 L. Jeanty ¹²³, J. Jejelava ^{149a,al}, P. Jenni ^{54,i}, C.E. Jessiman ³⁴, S. Jézéquel ⁴, C. Jia ^{62b}, J. Jia ¹⁴⁵,
 X. Jia ⁶¹, X. Jia ^{14a,14e}, Z. Jia ^{14c}, S. Jiggins ⁴⁸, J. Jimenez Pena ¹³, S. Jin ^{14c}, A. Jinaru ^{27b},
 O. Jinnouchi ¹⁵⁴, P. Johansson ¹³⁹, K.A. Johns ⁷, J.W. Johnson ¹³⁶, D.M. Jones ³², E. Jones ⁴⁸,
 P. Jones ³², R.W.L. Jones ⁹¹, T.J. Jones ⁹², H.L. Joos ^{55,36}, R. Joshi ¹¹⁹, J. Jovicevic ¹⁵,
 X. Ju ^{17a}, J.J. Junggeburth ^{103,v}, T. Junkermann ^{63a}, A. Juste Rozas ^{13,ad}, M.K. Juzek ⁸⁷,
 S. Kabana ^{137e}, A. Kaczmarzka ⁸⁷, M. Kado ¹¹⁰, H. Kagan ¹¹⁹, M. Kagan ¹⁴³, A. Kahn ⁴¹,
 A. Kahn ¹²⁸, C. Kahra ¹⁰⁰, T. Kaji ¹⁵³, E. Kajomovitz ¹⁵⁰, N. Kakati ¹⁶⁹, I. Kalaitzidou ⁵⁴,

C.W. Kalderon ²⁹, A. Kamenshchikov ¹⁵⁵, N.J. Kang ¹³⁶, D. Kar ^{33g}, K. Karava ¹²⁶, M.J. Kareem ^{156b}, E. Karentzos ⁵⁴, I. Karkanias ¹⁵², O. Karkout ¹¹⁴, S.N. Karpov ³⁸, Z.M. Karpova ³⁸, V. Kartvelishvili ⁹¹, A.N. Karyukhin ³⁷, E. Kasimi ¹⁵², J. Katzy ⁴⁸, S. Kaur ³⁴, K. Kawade ¹⁴⁰, M.P. Kawale ¹²⁰, C. Kawamoto ⁸⁸, T. Kawamoto ¹³⁵, E.F. Kay ³⁶, F.I. Kaya ¹⁵⁸, S. Kazakos ¹⁰⁷, V.F. Kazanin ³⁷, Y. Ke ¹⁴⁵, J.M. Keaveney ^{33a}, R. Keeler ¹⁶⁵, G.V. Kehris ⁶¹, J.S. Keller ³⁴, A.S. Kelly ⁹⁶, J.J. Kempster ¹⁴⁶, K.E. Kennedy ⁴¹, P.D. Kennedy ¹⁰⁰, O. Kepka ¹³¹, B.P. Kerridge ¹⁶⁷, S. Kersten ¹⁷¹, B.P. Kerševan ⁹³, S. Keshri ⁶⁶, L. Keszeghova ^{28a}, S. Ketabchi Haghighat ¹⁵⁵, R.A. Khan ¹²⁹, M. Khandoga ¹²⁷, A. Khanov ¹²¹, A.G. Kharlamov ³⁷, T. Kharlamova ³⁷, E.E. Khoda ¹³⁸, M. Kholodenko ³⁷, T.J. Khoo ¹⁸, G. Khorialuli ¹⁶⁶, J. Khubua ^{149b}, Y.A.R. Khwaira ⁶⁶, A. Kilgallon ¹²³, D.W. Kim ^{47a,47b}, Y.K. Kim ³⁹, N. Kimura ⁹⁶, M.K. Kingston ⁵⁵, A. Kirchhoff ⁵⁵, C. Kirfel ²⁴, F. Kirfel ²⁴, J. Kirk ¹³⁴, A.E. Kiryunin ¹¹⁰, C. Kitsaki ¹⁰, O. Kivernyk ²⁴, M. Klassen ^{63a}, C. Klein ³⁴, L. Klein ¹⁶⁶, M.H. Klein ¹⁰⁶, M. Klein ⁹², S.B. Klein ⁵⁶, U. Klein ⁹², P. Klimek ³⁶, A. Klimentov ²⁹, T. Klioutchnikova ³⁶, P. Kluit ¹¹⁴, S. Kluth ¹¹⁰, E. Kneringer ⁷⁹, T.M. Knight ¹⁵⁵, A. Knue ⁴⁹, R. Kobayashi ⁸⁸, D. Kobylanski ¹⁶⁹, S.F. Koch ¹²⁶, M. Kocian ¹⁴³, P. Kodyš ¹³³, D.M. Koeck ¹²³, P.T. Koenig ²⁴, T. Koffas ³⁴, O. Kolay ⁵⁰, M. Kolb ¹³⁵, I. Koletsou ⁴, T. Komarek ¹²², K. Köneke ⁵⁴, A.X.Y. Kong ¹, T. Kono ¹¹⁸, N. Konstantinidis ⁹⁶, P. Kontaxakis ⁵⁶, B. Konya ⁹⁸, R. Kopeliansky ⁶⁸, S. Koperny ^{86a}, K. Korcyl ⁸⁷, K. Kordas ^{152,f}, G. Koren ¹⁵¹, A. Korn ⁹⁶, S. Korn ⁵⁵, I. Korolkov ¹³, N. Korotkova ³⁷, B. Kortman ¹¹⁴, O. Kortner ¹¹⁰, S. Kortner ¹¹⁰, W.H. Kostecka ¹¹⁵, V.V. Kostyukhin ¹⁴¹, A. Kotsokechagia ¹³⁵, A. Kotwal ⁵¹, A. Koulouris ³⁶, A. Kourkoumeli-Charalampidi ^{73a,73b}, C. Kourkoumelis ⁹, E. Kourlitis ^{110,at}, O. Kovanda ¹⁴⁶, R. Kowalewski ¹⁶⁵, W. Kozanecki ¹³⁵, A.S. Kozhin ³⁷, V.A. Kramarenko ³⁷, G. Kramberger ⁹³, P. Kramer ¹⁰⁰, M.W. Krasny ¹²⁷, A. Krasznahorkay ³⁶, J.W. Kraus ¹⁷¹, J.A. Kremer ⁴⁸, T. Kresse ⁵⁰, J. Kretschmar ⁹², K. Kreul ¹⁸, P. Krieger ¹⁵⁵, S. Krishnamurthy ¹⁰³, M. Krivos ¹³³, K. Krizka ²⁰, K. Kroeninger ⁴⁹, H. Kroha ¹¹⁰, J. Kroll ¹³¹, J. Kroll ¹²⁸, K.S. Krowpman ¹⁰⁷, U. Kruchonak ³⁸, H. Krüger ²⁴, N. Krumnack ⁸¹, M.C. Kruse ⁵¹, J.A. Krzysiak ⁸⁷, O. Kuchinskaia ³⁷, S. Kuday ^{3a}, S. Kuehn ³⁶, R. Kuesters ⁵⁴, T. Kuhl ⁴⁸, V. Kukhtin ³⁸, Y. Kulchitsky ^{37,a}, S. Kuleshov ^{137d,137b}, M. Kumar ^{33g}, N. Kumari ⁴⁸, A. Kupco ¹³¹, T. Kupfer ⁴⁹, A. Kupich ³⁷, O. Kuprash ⁵⁴, H. Kurashige ⁸⁵, L.L. Kurchaninov ^{156a}, O. Kurdysh ⁶⁶, Y.A. Kurochkin ³⁷, A. Kurova ³⁷, M. Kuze ¹⁵⁴, A.K. Kvam ¹⁰³, J. Kvita ¹²², T. Kwan ¹⁰⁴, N.G. Kyriacou ¹⁰⁶, L.A.O. Laatu ¹⁰², C. Lacasta ¹⁶³, F. Lacava ^{75a,75b}, H. Lacker ¹⁸, D. Lacour ¹²⁷, N.N. Lad ⁹⁶, E. Ladygin ³⁸, B. Laforge ¹²⁷, T. Lagouri ^{137e}, F.Z. Lahbabi ^{35a}, S. Lai ⁵⁵, I.K. Lakomic ^{86a}, N. Lalloue ⁶⁰, J.E. Lambert ^{165,n}, S. Lammers ⁶⁸, W. Lampl ⁷, C. Lampoudis ^{152,f}, A.N. Lancaster ¹¹⁵, E. Lançon ²⁹, U. Landgraf ⁵⁴, M.P.J. Landon ⁹⁴, V.S. Lang ⁵⁴, R.J. Langenberg ¹⁰³, O.K.B. Langrekken ¹²⁵, A.J. Lankford ¹⁶⁰, F. Lanni ³⁶, K. Lantzsch ²⁴, A. Lanza ^{73a}, A. Lapertosa ^{57b,57a}, J.F. Laporte ¹³⁵, T. Lari ^{71a}, F. Lasagni Manghi ^{23b}, M. Lassnig ³⁶, V. Latonova ¹³¹, A. Laudrain ¹⁰⁰, A. Laurier ¹⁵⁰, S.D. Lawlor ¹³⁹, Z. Lawrence ¹⁰¹, R. Lazaridou ¹⁶⁷, M. Lazzaroni ^{71a,71b}, B. Le ¹⁰¹, E.M. Le Boulicaut ⁵¹, B. Leban ⁹³, A. Lebedev ⁸¹, M. LeBlanc ^{101,ar}, F. Ledroit-Guillon ⁶⁰, A.C.A. Lee ⁹⁶, S.C. Lee ¹⁴⁸, S. Lee ^{47a,47b}, T.F. Lee ⁹², L.L. Leeuw ^{33c}, H.P. Lefebvre ⁹⁵, M. Lefebvre ¹⁶⁵, C. Leggett ^{17a}, G. Lehmann Miotto ³⁶, M. Leigh ⁵⁶, W.A. Leight ¹⁰³, W. Leinonen ¹¹³, A. Leisos ^{152,ac}, M.A.L. Leite ^{83c}, C.E. Leitgeb ⁴⁸, R. Leitner ¹³³, K.J.C. Leney ⁴⁴, T. Lenz ²⁴, S. Leone ^{74a}, C. Leonidopoulos ⁵², A. Leopold ¹⁴⁴, C. Leroy ¹⁰⁸, R. Les ¹⁰⁷, C.G. Lester ³², M. Levchenko ³⁷, J. Levêque ⁴, D. Levin ¹⁰⁶, L.J. Levinson ¹⁶⁹, M.P. Lewicki ⁸⁷, D.J. Lewis ⁴, A. Li ⁵, B. Li ^{62b}, C. Li ^{62a}, C-Q. Li ^{62c}, H. Li ^{62a}, H. Li ^{62b}, H. Li ^{14c}, H. Li ^{14b}, H. Li ^{62b}, J. Li ^{62c}, K. Li ¹³⁸, L. Li ^{62c}, M. Li ^{14a,14e}, Q.Y. Li ^{62a}, S. Li ^{14a,14e}, S. Li ^{62d,62c,e}, T. Li ^{5,c}, X. Li ¹⁰⁴, Z. Li ¹²⁶, Z. Li ¹⁰⁴, Z. Li ⁹², Z. Li ^{14a,14e},

S. Liang^{14a,14e}, Z. Liang^{14a}, M. Liberatore^{135,am}, B. Liberti^{76a}, K. Lie^{64c}, J. Lieber Marin^{83b},
 H. Lien⁶⁸, K. Lin¹⁰⁷, R.E. Lindley⁷, J.H. Lindon², E. Lipeles¹²⁸, A. Lipniacka¹⁶,
 A. Lister¹⁶⁴, J.D. Little⁴, B. Liu^{14a}, B.X. Liu¹⁴², D. Liu^{62d,62c}, J.B. Liu^{62a}, J.K.K. Liu³²,
 K. Liu^{62d,62c}, M. Liu^{62a}, M.Y. Liu^{62a}, P. Liu^{14a}, Q. Liu^{62d,138,62c}, X. Liu^{62a}, Y. Liu^{14d,14e},
 Y.L. Liu^{62b}, Y.W. Liu^{62a}, J. Llorente Merino¹⁴², S.L. Lloyd⁹⁴, E.M. Lobodzinska⁴⁸,
 P. Loch⁷, T. Lohse¹⁸, K. Lohwasser¹³⁹, E. Loiacono⁴⁸, M. Lokajicek^{131,*}, J.D. Lomas²⁰,
 J.D. Long¹⁶², I. Longarini¹⁶⁰, L. Longo^{70a,70b}, R. Longo¹⁶², I. Lopez Paz⁶⁷,
 A. Lopez Solis⁴⁸, J. Lorenz¹⁰⁹, N. Lorenzo Martinez⁴, A.M. Lory¹⁰⁹, O. Loseva³⁷,
 X. Lou^{47a,47b}, X. Lou^{14a,14e}, A. Lounis⁶⁶, J. Love⁶, P.A. Love⁹¹, G. Lu^{14a,14e}, M. Lu⁸⁰,
 S. Lu¹²⁸, Y.J. Lu⁶⁵, H.J. Lubatti¹³⁸, C. Luci^{75a,75b}, F.L. Lucio Alves^{14c}, A. Lucotte⁶⁰,
 F. Luehring⁶⁸, I. Luise¹⁴⁵, O. Lukianchuk⁶⁶, O. Lundberg¹⁴⁴, B. Lund-Jensen¹⁴⁴,
 N.A. Luongo¹²³, M.S. Lutz¹⁵¹, A.B. Lux²⁵, D. Lynn²⁹, H. Lyons⁹², R. Lysak¹³¹,
 E. Lytken⁹⁸, V. Lyubushkin³⁸, T. Lyubushkina³⁸, M.M. Lyukova¹⁴⁵, H. Ma²⁹, K. Ma^{62a},
 L.L. Ma^{62b}, W. Ma^{62a}, Y. Ma¹²¹, D.M. Mac Donell¹⁶⁵, G. Maccarrone⁵³,
 J.C. MacDonald¹⁰⁰, P.C. Machado De Abreu Farias^{83b}, R. Madar⁴⁰, W.F. Mader⁵⁰,
 T. Madula⁹⁶, J. Maeda⁸⁵, T. Maeno²⁹, H. Maguire¹³⁹, V. Maiboroda¹³⁵,
 A. Maio^{130a,130b,130d}, K. Maj^{86a}, O. Majersky⁴⁸, S. Majewski¹²³, N. Makovec⁶⁶,
 V. Maksimovic¹⁵, B. Malaescu¹²⁷, Pa. Malecki⁸⁷, V.P. Maleev³⁷, F. Malek⁶⁰, M. Mali⁹³,
 D. Malito^{95,s}, U. Mallik⁸⁰, S. Maltezos¹⁰, S. Malyukov³⁸, J. Mamuzic¹³, G. Mancini⁵³,
 G. Manco^{73a,73b}, J.P. Mandalia⁹⁴, I. Mandić⁹³, L. Manhaes de Andrade Filho^{83a},
 I.M. Maniatis¹⁶⁹, J. Manjarres Ramos^{102,an}, D.C. Mankad¹⁶⁹, A. Mann¹⁰⁹, B. Mansoulie¹³⁵,
 S. Manzoni³⁶, L. Mao^{62c}, X. Mapekula^{33c}, A. Marantis^{152,ac}, G. Marchiori⁵,
 M. Marcisovsky¹³¹, C. Marcon^{71a,71b}, M. Marinescu²⁰, M. Marjanovic¹²⁰, E.J. Marshall⁹¹,
 Z. Marshall^{17a}, S. Marti-Garcia¹⁶³, T.A. Martin¹⁶⁷, V.J. Martin⁵², B. Martin dit Latour¹⁶,
 L. Martinelli^{75a,75b}, M. Martinez^{13,ad}, P. Martinez Agullo¹⁶³, V.I. Martinez Outschoorn¹⁰³,
 P. Martinez Suarez¹³, S. Martin-Haugh¹³⁴, V.S. Martoiu^{27b}, A.C. Martyniuk⁹⁶, A. Marzin³⁶,
 D. Mascione^{78a,78b}, L. Masetti¹⁰⁰, T. Mashimo¹⁵³, J. Masik¹⁰¹, A.L. Maslennikov³⁷,
 L. Massa^{23b}, P. Massarotti^{72a,72b}, P. Mastrandrea^{74a,74b}, A. Mastroberardino^{43b,43a},
 T. Masubuchi¹⁵³, T. Mathisen¹⁶¹, J. Matousek¹³³, N. Matsuzawa¹⁵³, J. Maurer^{27b}, B. Maček⁹³,
 D.A. Maximov³⁷, R. Mazini¹⁴⁸, I. Maznas¹⁵², M. Mazza¹⁰⁷, S.M. Mazza¹³⁶,
 E. Mazzeo^{71a,71b}, C. Mc Ginn²⁹, J.P. Mc Gowan¹⁰⁴, S.P. Mc Kee¹⁰⁶, E.F. McDonald¹⁰⁵,
 A.E. McDougall¹¹⁴, J.A. Mcfayden¹⁴⁶, R.P. McGovern¹²⁸, G. Mchedlidze^{149b},
 R.P. Mckenzie^{33g}, T.C. Mclachlan⁴⁸, D.J. Mclaughlin⁹⁶, S.J. McMahon¹³⁴,
 C.M. Mcpartland⁹², R.A. McPherson^{165,ai}, S. Mehlhase¹⁰⁹, A. Mehta⁹², D. Melini¹⁵⁰,
 B.R. Mellado Garcia^{33g}, A.H. Melo⁵⁵, F. Meloni⁴⁸, A.M. Mendes Jacques Da Costa¹⁰¹,
 H.Y. Meng¹⁵⁵, L. Meng⁹¹, S. Menke¹¹⁰, M. Mentink³⁶, E. Meoni^{43b,43a}, G. Mercado¹¹⁵,
 C. Merlassino¹²⁶, L. Merola^{72a,72b}, C. Meroni^{71a,71b}, G. Merz¹⁰⁶, O. Meshkov³⁷, J. Metcalfe⁶,
 A.S. Mete⁶, C. Meyer⁶⁸, J-P. Meyer¹³⁵, R.P. Middleton¹³⁴, L. Mijović⁵², G. Mikenberg¹⁶⁹,
 M. Mikestikova¹³¹, M. Mikuž⁹³, H. Mildner¹⁰⁰, A. Milic³⁶, C.D. Milke⁴⁴, D.W. Miller³⁹,
 L.S. Miller³⁴, A. Milov¹⁶⁹, D.A. Milstead^{47a,47b}, T. Min^{14c}, A.A. Minaenko³⁷,
 I.A. Minashvili^{149b}, L. Mince⁵⁹, A.I. Mincer¹¹⁷, B. Mindur^{86a}, M. Mineev³⁸, Y. Mino⁸⁸,
 L.M. Mir¹³, M. Miralles Lopez¹⁶³, M. Mironova^{17a}, A. Mishima¹⁵³, M.C. Missio¹¹³,
 A. Mitra¹⁶⁷, V.A. Mitsou¹⁶³, Y. Mitsumori¹¹¹, O. Miu¹⁵⁵, P.S. Miyagawa⁹⁴,
 T. Mkrtchyan^{63a}, M. Mlinarevic⁹⁶, T. Mlinarevic⁹⁶, M. Mlynarikova³⁶, S. Mobius¹⁹,
 P. Moder⁴⁸, P. Mogg¹⁰⁹, A.F. Mohammed^{14a,14e}, S. Mohapatra⁴¹, G. Mokgatitwane^{33g},
 L. Moleri¹⁶⁹, B. Mondal¹⁴¹, S. Mondal¹³², G. Monig¹⁴⁶, K. Mönig⁴⁸, E. Monnier¹⁰²,
 L. Monsonis Romero¹⁶³, J. Montejo Berlingen¹³, M. Montella¹¹⁹, F. Montekali^{77a,77b},

F. Monticelli ^{id90}, S. Monzani ^{id69a,69c}, N. Morange ^{id66}, A.L. Moreira De Carvalho ^{id130a}, M. Moreno Llácer ^{id163}, C. Moreno Martinez ^{id56}, P. Moretini ^{id57b}, S. Morgenstern ^{id36}, M. Morii ^{id61}, M. Morinaga ^{id153}, A.K. Morley ^{id36}, F. Morodei ^{id75a,75b}, L. Morvaj ^{id36}, P. Moschovakos ^{id36}, B. Moser ^{id36}, M. Mosidze ^{id149b}, T. Moskalets ^{id54}, P. Moskvitina ^{id113}, J. Moss ^{id31,p}, E.J.W. Moyses ^{id103}, O. Mtintsilana ^{id33g}, S. Muanza ^{id102}, J. Mueller ^{id129}, D. Muenstermann ^{id91}, R. Müller ^{id19}, G.A. Mullier ^{id161}, A.J. Mullin ^{id32}, J.J. Mullin ^{id128}, D.P. Mungo ^{id155}, D. Munoz Perez ^{id163}, F.J. Munoz Sanchez ^{id101}, M. Murin ^{id101}, W.J. Murray ^{id167,134}, A. Murrone ^{id71a,71b}, M. Muškinja ^{id17a}, C. Mwewa ^{id29}, A.G. Myagkov ^{id37,a}, A.J. Myers ^{id8}, G. Myers ^{id68}, M. Myska ^{id132}, B.P. Nachman ^{id17a}, O. Nackenhorst ^{id49}, A. Nag ^{id50}, K. Nagai ^{id126}, K. Nagano ^{id84}, J.L. Nagle ^{id29,ay}, E. Nagy ^{id102}, A.M. Nairz ^{id36}, Y. Nakahama ^{id84}, K. Nakamura ^{id84}, K. Nakkalil ^{id5}, H. Nanjo ^{id124}, R. Narayan ^{id44}, E.A. Narayanan ^{id112}, I. Naryshkin ^{id37}, M. Naseri ^{id34}, S. Nasri ^{id159}, C. Nass ^{id24}, G. Navarro ^{id22a}, J. Navarro-Gonzalez ^{id163}, R. Nayak ^{id151}, A. Nayaz ^{id18}, P.Y. Nechaeva ^{id37}, F. Nechansky ^{id48}, L. Nedic ^{id126}, T.J. Neep ^{id20}, A. Negri ^{id73a,73b}, M. Negrini ^{id23b}, C. Nellist ^{id114}, C. Nelson ^{id104}, K. Nelson ^{id106}, S. Nemecek ^{id131}, M. Nessi ^{id36,j}, M.S. Neubauer ^{id162}, F. Neuhaus ^{id100}, J. Neundorff ^{id48}, R. Newhouse ^{id164}, P.R. Newman ^{id20}, C.W. Ng ^{id129}, Y.W.Y. Ng ^{id48}, B. Ngair ^{id35e}, H.D.N. Nguyen ^{id108}, R.B. Nickerson ^{id126}, R. Nicolaidou ^{id135}, J. Nielsen ^{id136}, M. Niemeyer ^{id55}, J. Niermann ^{id55,36}, N. Nikiforou ^{id36}, V. Nikolaenko ^{id37,a}, I. Nikolic-Audit ^{id127}, K. Nikolopoulos ^{id20}, P. Nilsson ^{id29}, I. Ninca ^{id48}, H.R. Nindhito ^{id56}, G. Ninio ^{id151}, A. Nisati ^{id75a}, N. Nishu ^{id2}, R. Nisius ^{id110}, J-E. Nitschke ^{id50}, E.K. Nkadimeng ^{id33g}, T. Nobe ^{id153}, D.L. Noel ^{id32}, T. Nommensen ^{id147}, M.B. Norfolk ^{id139}, R.R.B. Norisam ^{id96}, B.J. Norman ^{id34}, J. Novak ^{id93}, T. Novak ^{id48}, L. Novotny ^{id132}, R. Novotny ^{id112}, L. Nozka ^{id122}, K. Ntekas ^{id160}, N.M.J. Nunes De Moura Junior ^{id83b}, E. Nurse ^{id96}, J. Ocariz ^{id127}, A. Ochi ^{id85}, I. Ochoa ^{id130a}, S. Oerdek ^{id48,y}, J.T. Offermann ^{id39}, A. Ogrodnik ^{id133}, A. Oh ^{id101}, C.C. Ohm ^{id144}, H. Oide ^{id84}, R. Oishi ^{id153}, M.L. Ojeda ^{id48}, M.W. O'Keefe ^{id92}, Y. Okumura ^{id153}, L.F. Oleiro Seabra ^{id130a}, S.A. Olivares Pino ^{id137d}, D. Oliveira Damazio ^{id29}, D. Oliveira Goncalves ^{id83a}, J.L. Oliver ^{id160}, Ö.O. Öncel ^{id54}, A.P. O'Neill ^{id19}, A. Onofre ^{id130a,130e}, P.U.E. Onyisi ^{id11}, M.J. Oreglia ^{id39}, G.E. Orellana ^{id90}, D. Orestano ^{id77a,77b}, N. Orlando ^{id13}, R.S. Orr ^{id155}, V. O'Shea ^{id59}, L.M. Osojnak ^{id128}, R. Ospanov ^{id62a}, G. Otero y Garzon ^{id30}, H. Otono ^{id89}, P.S. Ott ^{id63a}, G.J. Ottino ^{id17a}, M. Ouchrif ^{id35d}, J. Ouellette ^{id29}, F. Ould-Saada ^{id125}, M. Owen ^{id59}, R.E. Owen ^{id134}, K.Y. Oyulmaz ^{id21a}, V.E. Ozcan ^{id21a}, F. Ozturk ^{id87}, N. Ozturk ^{id8}, S. Ozturk ^{id82}, H.A. Pacey ^{id126}, A. Pacheco Pages ^{id13}, C. Padilla Aranda ^{id13}, G. Padovano ^{id75a,75b}, S. Pagan Griso ^{id17a}, G. Palacino ^{id68}, A. Palazzo ^{id70a,70b}, S. Palestini ^{id36}, J. Pan ^{id172}, T. Pan ^{id64a}, D.K. Panchal ^{id11}, C.E. Pandini ^{id114}, J.G. Panduro Vazquez ^{id95}, H.D. Pandya ^{id1}, H. Pang ^{id14b}, P. Pani ^{id48}, G. Panizzo ^{id69a,69c}, L. Paolozzi ^{id56}, C. Papadatos ^{id108}, S. Parajuli ^{id44}, A. Paramonov ^{id36}, C. Paraskevopoulos ^{id10}, D. Paredes Hernandez ^{id64b}, K.R. Park ^{id41}, T.H. Park ^{id155}, M.A. Parker ^{id32}, F. Parodi ^{id57b,57a}, E.W. Parrish ^{id115}, V.A. Parrish ^{id52}, J.A. Parsons ^{id41}, U. Parzefall ^{id54}, B. Pascual Dias ^{id108}, L. Pascual Dominguez ^{id151}, E. Pasqualucci ^{id75a}, S. Passaggio ^{id57b}, F. Pastore ^{id95}, P. Pasuwan ^{id47a,47b}, P. Patel ^{id87}, U.M. Patel ^{id51}, J.R. Pater ^{id101}, T. Pauly ^{id36}, J. Pearkes ^{id143}, M. Pedersen ^{id125}, R. Pedro ^{id130a}, S.V. Peleganchuk ^{id37}, O. Penc ^{id36}, E.A. Pender ^{id52}, K.E. Pensi ^{id109}, M. Penzin ^{id37}, B.S. Peralva ^{id83d}, A.P. Pereira Peixoto ^{id60}, L. Pereira Sanchez ^{id47a,47b}, D.V. Perepelitsa ^{id29,ay}, E. Perez Codina ^{id156a}, M. Perganti ^{id10}, L. Perini ^{id71a,71b,*}, H. Pernegger ^{id36}, O. Perrin ^{id40}, K. Peters ^{id48}, R.F.Y. Peters ^{id101}, B.A. Petersen ^{id36}, T.C. Petersen ^{id42}, E. Petit ^{id102}, V. Petousis ^{id132}, C. Petridou ^{id152,f}, A. Petrukhin ^{id141}, M. Pettee ^{id17a}, N.E. Pettersson ^{id36}, A. Petukhov ^{id37}, K. Petukhova ^{id133}, R. Pezoa ^{id137f}, L. Pezzotti ^{id36}, G. Pezzullo ^{id172}, T.M. Pham ^{id170}, T. Pham ^{id105}, P.W. Phillips ^{id134}, G. Piacquadio ^{id145}, E. Pianori ^{id17a}, F. Piazza ^{id123}, R. Piegai ^{id30}, D. Pietreanu ^{id27b}, A.D. Pilkington ^{id101}, M. Pinamonti ^{id69a,69c}, J.L. Pinfeld ^{id2}, B.C. Pinheiro Pereira ^{id130a}, A.E. Pinto Pinoargote ^{id100,135}, L. Pintucci ^{id69a,69c}, K.M. Piper ^{id146},

A. Pirttikoski ⁵⁶, D.A. Pizzi ³⁴, L. Pizzimento ^{64b}, A. Pizzini ¹¹⁴, M.-A. Pleier ²⁹, V. Plesanovs ⁵⁴,
 V. Pleskot ¹³³, E. Plotnikova ³⁸, G. Poddar ⁴, R. Poettgen ⁹⁸, L. Poggioli ¹²⁷, I. Pokharel ⁵⁵,
 S. Polacek ¹³³, G. Polesello ^{73a}, A. Poley ^{142,156a}, R. Polifka ¹³², A. Polini ^{23b}, C.S. Pollard ¹⁶⁷,
 Z.B. Pollock ¹¹⁹, V. Polychronakos ²⁹, E. Pompa Pacchi ^{75a,75b}, D. Ponomarenko ¹¹³,
 L. Pontecorvo ³⁶, S. Popa ^{27a}, G.A. Popeneciu ^{27d}, A. Poreba ³⁶, D.M. Portillo Quintero ^{156a},
 S. Pospisil ¹³², M.A. Postill ¹³⁹, P. Postolache ^{27c}, K. Potamianos ¹⁶⁷, P.A. Potepa ^{86a},
 I.N. Potrap ³⁸, C.J. Potter ³², H. Potti ¹, T. Poulsen ⁴⁸, J. Poveda ¹⁶³, M.E. Pozo Astigarraga ³⁶,
 A. Prades Ibanez ¹⁶³, J. Pretel ⁵⁴, D. Price ¹⁰¹, M. Primavera ^{70a}, M.A. Principe Martin ⁹⁹,
 R. Privara ¹²², T. Procter ⁵⁹, M.L. Proffitt ¹³⁸, N. Proklova ¹²⁸, K. Prokofiev ^{64c}, G. Proto ¹¹⁰,
 S. Protopopescu ²⁹, J. Proudfoot ⁶, M. Przybycien ^{86a}, W.W. Przygoda ^{86b}, J.E. Puddefoot ¹³⁹,
 D. Pudzha ³⁷, D. Pyatiiybyantseva ³⁷, J. Qian ¹⁰⁶, D. Qichen ¹⁰¹, Y. Qin ¹⁰¹, T. Qiu ⁵²,
 A. Quadt ⁵⁵, M. Queitsch-Maitland ¹⁰¹, G. Quetant ⁵⁶, R.P. Quinn ¹⁶⁴, G. Rabanal Bolanos ⁶¹,
 D. Rafanoharana ⁵⁴, F. Ragusa ^{71a,71b}, J.L. Rainbolt ³⁹, J.A. Raine ⁵⁶, S. Rajagopalan ²⁹,
 E. Ramakoti ³⁷, I.A. Ramirez-Berend ³⁴, K. Ran ^{48,14e}, N.P. Rapheeha ^{33g}, H. Rasheed ^{27b},
 V. Raskina ¹²⁷, D.F. Rassloff ^{63a}, S. Rave ¹⁰⁰, B. Ravina ⁵⁵, I. Ravinovich ¹⁶⁹, M. Raymond ³⁶,
 A.L. Read ¹²⁵, N.P. Readioff ¹³⁹, D.M. Rebutzi ^{73a,73b}, G. Redlinger ²⁹, A.S. Reed ¹¹⁰,
 K. Reeves ²⁶, J.A. Reidelsturz ^{171,aa}, D. Reikher ¹⁵¹, A. Rej ^{49,z}, C. Rembser ³⁶, A. Renardi ⁴⁸,
 M. Renda ^{27b}, M.B. Rendel ¹¹⁰, F. Renner ⁴⁸, A.G. Rennie ¹⁶⁰, A.L. Rescia ⁴⁸, S. Resconi ^{71a},
 M. Ressegotti ^{57b,57a}, S. Rettie ³⁶, J.G. Reyes Rivera ¹⁰⁷, E. Reynolds ^{17a}, O.L. Rezanova ³⁷,
 P. Reznicek ¹³³, N. Ribaric ⁹¹, E. Ricci ^{78a,78b}, R. Richter ¹¹⁰, S. Richter ^{47a,47b},
 E. Richter-Was ^{86b}, M. Ridel ¹²⁷, S. Ridouani ^{35d}, P. Rieck ¹¹⁷, P. Riedler ³⁶, E.M. Riefel ^{47a,47b},
 J.O. Rieger ¹¹⁴, M. Rijssenbeek ¹⁴⁵, A. Rimoldi ^{73a,73b}, M. Rimoldi ³⁶, L. Rinaldi ^{23b,23a},
 T.T. Rinn ²⁹, M.P. Rinnagel ¹⁰⁹, G. Ripellino ¹⁶¹, I. Riu ¹³, P. Rivadeneira ⁴⁸,
 J.C. Rivera Vergara ¹⁶⁵, F. Rizatdinova ¹²¹, E. Rizvi ⁹⁴, B.A. Roberts ¹⁶⁷, B.R. Roberts ^{17a},
 S.H. Robertson ^{104,ai}, D. Robinson ³², C.M. Robles Gajardo ^{137f}, M. Robles Manzano ¹⁰⁰,
 A. Robson ⁵⁹, A. Rocchi ^{76a,76b}, C. Roda ^{74a,74b}, S. Rodriguez Bosca ^{63a}, Y. Rodriguez Garcia ^{22a},
 A. Rodriguez Rodriguez ⁵⁴, A.M. Rodríguez Vera ^{156b}, S. Roe ³⁶, J.T. Roemer ¹⁶⁰,
 A.R. Roepe-Gier ¹³⁶, J. Roggel ¹⁷¹, O. Røhne ¹²⁵, R.A. Rojas ¹⁰³, C.P.A. Roland ¹²⁷,
 J. Roloff ²⁹, A. Romaniouk ³⁷, E. Romano ^{73a,73b}, M. Romano ^{23b}, A.C. Romero Hernandez ¹⁶²,
 N. Rompotis ⁹², L. Roos ¹²⁷, S. Rosati ^{75a}, B.J. Rosser ³⁹, E. Rossi ¹²⁶, E. Rossi ^{72a,72b},
 L.P. Rossi ^{57b}, L. Rossini ⁵⁴, R. Rosten ¹¹⁹, M. Rotaru ^{27b}, B. Rottler ⁵⁴, C. Rougier ^{102,an},
 D. Rousseau ⁶⁶, D. Rousso ³², A. Roy ¹⁶², S. Roy-Garand ¹⁵⁵, A. Rozanov ¹⁰²,
 Z.M.A. Rozario ⁵⁹, Y. Rozen ¹⁵⁰, X. Ruan ^{33g}, A. Rubio Jimenez ¹⁶³, A.J. Ruby ⁹²,
 V.H. Ruelas Rivera ¹⁸, T.A. Ruggeri ¹, A. Ruggiero ¹²⁶, A. Ruiz-Martinez ¹⁶³, A. Rummler ³⁶,
 Z. Rurikova ⁵⁴, N.A. Rusakovich ³⁸, H.L. Russell ¹⁶⁵, G. Russo ^{75a,75b}, J.P. Rutherford ⁷,
 S. Rutherford Colmenares ³², K. Rybacki ⁹¹, M. Rybar ¹³³, E.B. Rye ¹²⁵, A. Ryzhov ⁴⁴,
 J.A. Sabater Iglesias ⁵⁶, P. Sabatini ¹⁶³, L. Sabetta ^{75a,75b}, H.F-W. Sadrozinski ¹³⁶,
 F. Safai Tehrani ^{75a}, B. Safarzadeh Samani ¹³⁴, M. Safdari ¹⁴³, S. Saha ¹⁶⁵, M. Sahinsoy ¹¹⁰,
 M. Saimpert ¹³⁵, M. Saito ¹⁵³, T. Saito ¹⁵³, D. Salamani ³⁶, A. Salnikov ¹⁴³, J. Salt ¹⁶³,
 A. Salvador Salas ¹⁵¹, D. Salvatore ^{43b,43a}, F. Salvatore ¹⁴⁶, A. Salzburger ³⁶, D. Sammel ⁵⁴,
 D. Sampsonidis ^{152,f}, D. Sampsonidou ¹²³, J. Sánchez ¹⁶³, A. Sanchez Pineda ⁴,
 V. Sanchez Sebastian ¹⁶³, H. Sandaker ¹²⁵, C.O. Sander ⁴⁸, J.A. Sandesara ¹⁰³, M. Sandhoff ¹⁷¹,
 C. Sandoval ^{22b}, D.P.C. Sankey ¹³⁴, T. Sano ⁸⁸, A. Sansoni ⁵³, L. Santi ^{75a,75b}, C. Santoni ⁴⁰,
 H. Santos ^{130a,130b}, S.N. Santpur ^{17a}, A. Santra ¹⁶⁹, K.A. Saoucha ^{116b}, J.G. Saraiva ^{130a,130d},
 J. Sardain ⁷, O. Sasaki ⁸⁴, K. Sato ¹⁵⁷, C. Sauer ^{63b}, F. Sauerburger ⁵⁴, E. Sauvan ⁴,
 P. Savard ^{155,av}, R. Sawada ¹⁵³, C. Sawyer ¹³⁴, L. Sawyer ⁹⁷, I. Sayago Galvan ¹⁶³, C. Sbarra ^{23b},
 A. Sbrizzi ^{23b,23a}, T. Scanlon ⁹⁶, J. Schaarschmidt ¹³⁸, P. Schacht ¹¹⁰, U. Schäfer ¹⁰⁰,

A.C. Schaffer [ID 66,44](#), D. Schaile [ID 109](#), R.D. Schamberger [ID 145](#), C. Scharf [ID 18](#), M.M. Schefer [ID 19](#),
 V.A. Schegelsky [ID 37](#), D. Scheirich [ID 133](#), F. Schenck [ID 18](#), M. Schernau [ID 160](#), C. Scheulen [ID 55](#),
 C. Schiavi [ID 57b,57a](#), E.J. Schioppa [ID 70a,70b](#), M. Schioppa [ID 43b,43a](#), B. Schlag [ID 143,t](#), K.E. Schleicher [ID 54](#),
 S. Schlenker [ID 36](#), J. Schmeing [ID 171](#), M.A. Schmidt [ID 171](#), K. Schmieden [ID 100](#), C. Schmitt [ID 100](#),
 N. Schmitt [ID 100](#), S. Schmitt [ID 48](#), L. Schoeffel [ID 135](#), A. Schoening [ID 63b](#), P.G. Scholer [ID 54](#), E. Schopf [ID 126](#),
 M. Schott [ID 100](#), J. Schovancova [ID 36](#), S. Schramm [ID 56](#), F. Schroeder [ID 171](#), T. Schroer [ID 56](#),
 H-C. Schultz-Coulon [ID 63a](#), M. Schumacher [ID 54](#), B.A. Schumm [ID 136](#), Ph. Schune [ID 135](#), A.J. Schuy [ID 138](#),
 H.R. Schwartz [ID 136](#), A. Schwartzman [ID 143](#), T.A. Schwarz [ID 106](#), Ph. Schwemling [ID 135](#),
 R. Schwienhorst [ID 107](#), A. Sciandra [ID 136](#), G. Sciolla [ID 26](#), F. Scuri [ID 74a](#), C.D. Sebastiani [ID 92](#),
 K. Sedlaczek [ID 115](#), P. Seema [ID 18](#), S.C. Seidel [ID 112](#), A. Seiden [ID 136](#), B.D. Seidlitz [ID 41](#), C. Seitz [ID 48](#),
 J.M. Seixas [ID 83b](#), G. Sekhniaidze [ID 72a](#), S.J. Sekula [ID 44](#), L. Selem [ID 60](#), N. Semprini-Cesari [ID 23b,23a](#),
 D. Sengupta [ID 56](#), V. Senthilkumar [ID 163](#), L. Serin [ID 66](#), L. Serkin [ID 69a,69b](#), M. Sessa [ID 76a,76b](#),
 H. Severini [ID 120](#), F. Sforza [ID 57b,57a](#), A. Sfyrta [ID 56](#), E. Shabalina [ID 55](#), R. Shaheen [ID 144](#),
 J.D. Shahinian [ID 128](#), D. Shaked Renous [ID 169](#), L.Y. Shan [ID 14a](#), M. Shapiro [ID 17a](#), A. Sharma [ID 36](#),
 A.S. Sharma [ID 164](#), P. Sharma [ID 80](#), S. Sharma [ID 48](#), P.B. Shatalov [ID 37](#), K. Shaw [ID 146](#), S.M. Shaw [ID 101](#),
 A. Shcherbakova [ID 37](#), Q. Shen [ID 62c,5](#), P. Sherwood [ID 96](#), L. Shi [ID 96](#), X. Shi [ID 14a](#), C.O. Shimmin [ID 172](#),
 J.D. Shinner [ID 95](#), I.P.J. Shipsey [ID 126](#), S. Shirabe [ID 56,j](#), M. Shiyakova [ID 38,ag](#), J. Shlomi [ID 169](#),
 M.J. Shochet [ID 39](#), J. Shojaii [ID 105](#), D.R. Shope [ID 125](#), B. Shrestha [ID 120](#), S. Shrestha [ID 119,az](#),
 E.M. Shrif [ID 33g](#), M.J. Shroff [ID 165](#), P. Sicho [ID 131](#), A.M. Sickles [ID 162](#), E. Sideras Haddad [ID 33g](#),
 A. Sidoti [ID 23b](#), F. Siegert [ID 50](#), Dj. Sijacki [ID 15](#), R. Sikora [ID 86a](#), F. Sili [ID 90](#), J.M. Silva [ID 20](#),
 M.V. Silva Oliveira [ID 29](#), S.B. Silverstein [ID 47a](#), S. Simion [ID 66](#), R. Simoniello [ID 36](#), E.L. Simpson [ID 59](#),
 H. Simpson [ID 146](#), L.R. Simpson [ID 106](#), N.D. Simpson [ID 98](#), S. Simsek [ID 82](#), S. Sindhu [ID 55](#), P. Sinervo [ID 155](#),
 S. Singh [ID 155](#), S. Sinha [ID 48](#), S. Sinha [ID 101](#), M. Sioli [ID 23b,23a](#), I. Siral [ID 36](#), E. Sitnikova [ID 48](#),
 S.Yu. Sivoklov [ID 37,*](#), J. Sjölin [ID 47a,47b](#), A. Skaf [ID 55](#), E. Skorda [ID 20,aq](#), P. Skubic [ID 120](#),
 M. Slawinska [ID 87](#), V. Smakhtin [ID 169](#), B.H. Smart [ID 134](#), J. Smiesko [ID 36](#), S.Yu. Smirnov [ID 37](#), Y. Smirnov [ID 37](#),
 L.N. Smirnova [ID 37,a](#), O. Smirnova [ID 98](#), A.C. Smith [ID 41](#), E.A. Smith [ID 39](#), H.A. Smith [ID 126](#),
 J.L. Smith [ID 92](#), R. Smith [ID 143](#), M. Smizanska [ID 91](#), K. Smolek [ID 132](#), A.A. Snesarev [ID 37](#), S.R. Snider [ID 155](#),
 H.L. Snoek [ID 114](#), S. Snyder [ID 29](#), R. Sobie [ID 165,ai](#), A. Soffer [ID 151](#), C.A. Solans Sanchez [ID 36](#),
 E.Yu. Soldatov [ID 37](#), U. Soldevila [ID 163](#), A.A. Solodkov [ID 37](#), S. Solomon [ID 26](#), A. Soloshenko [ID 38](#),
 K. Solovieva [ID 54](#), O.V. Solovyanov [ID 40](#), V. Solovyev [ID 37](#), P. Sommer [ID 36](#), A. Sonay [ID 13](#),
 W.Y. Song [ID 156b](#), J.M. Sonneveld [ID 114](#), A. Sopczak [ID 132](#), A.L. Sopio [ID 96](#), F. Sopkova [ID 28b](#),
 I.R. Sotarriva Alvarez [ID 154](#), V. Sothilingam [ID 63a](#), O.J. Soto Sandoval [ID 137c,137b](#), S. Sottocornola [ID 68](#),
 R. Soualah [ID 116b](#), Z. Soumami [ID 35e](#), D. South [ID 48](#), N. Soybelman [ID 169](#), S. Spagnolo [ID 70a,70b](#),
 M. Spalla [ID 110](#), D. Sperlich [ID 54](#), G. Spigo [ID 36](#), S. Spinali [ID 91](#), D.P. Spiteri [ID 59](#), M. Spousta [ID 133](#),
 E.J. Staats [ID 34](#), A. Stabile [ID 71a,71b](#), R. Stamen [ID 63a](#), A. Stampekis [ID 20](#), M. Standke [ID 24](#), E. Stanecka [ID 87](#),
 M.V. Stange [ID 50](#), B. Stanislaus [ID 17a](#), M.M. Stanitzki [ID 48](#), B. Stapf [ID 48](#), E.A. Starchenko [ID 37](#),
 G.H. Stark [ID 136](#), J. Stark [ID 102,an](#), D.M. Starko [ID 156b](#), P. Staroba [ID 131](#), P. Starovoitov [ID 63a](#), S. Stärz [ID 104](#),
 R. Staszewski [ID 87](#), G. Stavropoulos [ID 46](#), J. Steentoft [ID 161](#), P. Steinberg [ID 29](#), B. Stelzer [ID 142,156a](#),
 H.J. Stelzer [ID 129](#), O. Stelzer-Chilton [ID 156a](#), H. Stenzel [ID 58](#), T.J. Stevenson [ID 146](#), G.A. Stewart [ID 36](#),
 J.R. Stewart [ID 121](#), M.C. Stockton [ID 36](#), G. Stoicea [ID 27b](#), M. Stolarski [ID 130a](#), S. Stonjek [ID 110](#),
 A. Straessner [ID 50](#), J. Strandberg [ID 144](#), S. Strandberg [ID 47a,47b](#), M. Stratmann [ID 171](#), M. Strauss [ID 120](#),
 T. Strebler [ID 102](#), P. Strizenc [ID 28b](#), R. Ströhmer [ID 166](#), D.M. Strom [ID 123](#), L.R. Strom [ID 48](#),
 R. Stroynowski [ID 44](#), A. Strubig [ID 47a,47b](#), S.A. Stucci [ID 29](#), B. Stugu [ID 16](#), J. Stupak [ID 120](#), N.A. Styles [ID 48](#),
 D. Su [ID 143](#), S. Su [ID 62a](#), W. Su [ID 62d](#), X. Su [ID 62a,66](#), K. Sugizaki [ID 153](#), V.V. Sulin [ID 37](#), M.J. Sullivan [ID 92](#),
 D.M.S. Sultan [ID 78a,78b](#), L. Sultanaliyeva [ID 37](#), S. Sultansoy [ID 3b](#), T. Sumida [ID 88](#), S. Sun [ID 106](#), S. Sun [ID 170](#),
 O. Sunneborn Gudnadottir [ID 161](#), N. Sur [ID 102](#), M.R. Sutton [ID 146](#), H. Suzuki [ID 157](#), M. Svatos [ID 131](#),
 M. Swiatlowski [ID 156a](#), T. Swirski [ID 166](#), I. Sykora [ID 28a](#), M. Sykora [ID 133](#), T. Sykora [ID 133](#), D. Ta [ID 100](#),

K. Tackmann [ID](#)^{48,ae}, A. Taffard [ID](#)¹⁶⁰, R. Tafirout [ID](#)^{156a}, J.S. Tafoya Vargas [ID](#)⁶⁶, E.P. Takeva [ID](#)⁵²,
 Y. Takubo [ID](#)⁸⁴, M. Talby [ID](#)¹⁰², A.A. Talyshev [ID](#)³⁷, K.C. Tam [ID](#)^{64b}, N.M. Tamir [ID](#)¹⁵¹, A. Tanaka [ID](#)¹⁵³,
 J. Tanaka [ID](#)¹⁵³, R. Tanaka [ID](#)⁶⁶, M. Tanasini [ID](#)^{57b,57a}, Z. Tao [ID](#)¹⁶⁴, S. Tapia Araya [ID](#)^{137f},
 S. Tapprogge [ID](#)¹⁰⁰, A. Tarek Abouelfadl Mohamed [ID](#)¹⁰⁷, S. Tarem [ID](#)¹⁵⁰, K. Tariq [ID](#)^{14a}, G. Tarna [ID](#)^{102,27b},
 G.F. Tartarelli [ID](#)^{71a}, P. Tas [ID](#)¹³³, M. Tasevsky [ID](#)¹³¹, E. Tassi [ID](#)^{43b,43a}, A.C. Tate [ID](#)¹⁶², G. Tateno [ID](#)¹⁵³,
 Y. Tayalati [ID](#)^{35e,ah}, G.N. Taylor [ID](#)¹⁰⁵, W. Taylor [ID](#)^{156b}, A.S. Tee [ID](#)¹⁷⁰, R. Teixeira De Lima [ID](#)¹⁴³,
 P. Teixeira-Dias [ID](#)⁹⁵, J.J. Teoh [ID](#)¹⁵⁵, K. Terashi [ID](#)¹⁵³, J. Terron [ID](#)⁹⁹, S. Terzo [ID](#)¹³, M. Testa [ID](#)⁵³,
 R.J. Teuscher [ID](#)^{155,ai}, A. Thaler [ID](#)⁷⁹, O. Theiner [ID](#)⁵⁶, N. Themistokleous [ID](#)⁵², T. Theveneaux-Pelzer [ID](#)¹⁰²,
 O. Thielmann [ID](#)¹⁷¹, D.W. Thomas [ID](#)⁹⁵, J.P. Thomas [ID](#)²⁰, E.A. Thompson [ID](#)^{17a}, P.D. Thompson [ID](#)²⁰,
 E. Thomson [ID](#)¹²⁸, Y. Tian [ID](#)⁵⁵, V. Tikhomirov [ID](#)^{37,a}, Yu.A. Tikhonov [ID](#)³⁷, S. Timoshenko [ID](#)³⁷,
 D. Timoshyn [ID](#)¹³³, E.X.L. Ting [ID](#)¹, P. Tipton [ID](#)¹⁷², S.H. Tlou [ID](#)^{33g}, A. Tnourji [ID](#)⁴⁰, K. Todome [ID](#)¹⁵⁴,
 S. Todorova-Nova [ID](#)¹³³, S. Todt [ID](#)⁵⁰, M. Togawa [ID](#)⁸⁴, J. Tojo [ID](#)⁸⁹, S. Tokár [ID](#)^{28a}, K. Tokushuku [ID](#)⁸⁴,
 O. Toldaiev [ID](#)⁶⁸, R. Tombs [ID](#)³², M. Tomoto [ID](#)^{84,111}, L. Tompkins [ID](#)^{143,t}, K.W. Topolnicki [ID](#)^{86b},
 E. Torrence [ID](#)¹²³, H. Torres [ID](#)^{102,an}, E. Torró Pastor [ID](#)¹⁶³, M. Toscani [ID](#)³⁰, C. Tosciri [ID](#)³⁹, M. Tost [ID](#)¹¹,
 D.R. Tovey [ID](#)¹³⁹, A. Traeet [ID](#)¹⁶, I.S. Trandafir [ID](#)^{27b}, T. Trefzger [ID](#)¹⁶⁶, A. Tricoli [ID](#)²⁹, I.M. Trigger [ID](#)^{156a},
 S. Trincaz-Duvoid [ID](#)¹²⁷, D.A. Trischuk [ID](#)²⁶, B. Trocmé [ID](#)⁶⁰, C. Troncon [ID](#)^{71a}, L. Truong [ID](#)^{33c},
 M. Trzebinski [ID](#)⁸⁷, A. Trzupiek [ID](#)⁸⁷, F. Tsai [ID](#)¹⁴⁵, M. Tsai [ID](#)¹⁰⁶, A. Tsiamis [ID](#)^{152,f}, P.V. Tsiarehka [ID](#)³⁷,
 S. Tsigaridas [ID](#)^{156a}, A. Tsirigotis [ID](#)^{152,ac}, V. Tsiskaridze [ID](#)¹⁵⁵, E.G. Tskhadadze [ID](#)^{149a},
 M. Tsopoulou [ID](#)^{152,f}, Y. Tsujikawa [ID](#)⁸⁸, I.I. Tsukerman [ID](#)³⁷, V. Tsulaia [ID](#)^{17a}, S. Tsuno [ID](#)⁸⁴, O. Tsur [ID](#)¹⁵⁰,
 K. Tsur [ID](#)¹¹⁸, D. Tsybychev [ID](#)¹⁴⁵, Y. Tu [ID](#)^{64b}, A. Tudorache [ID](#)^{27b}, V. Tudorache [ID](#)^{27b}, A.N. Tuna [ID](#)³⁶,
 S. Turchikhin [ID](#)^{57b,57a}, I. Turk Cakir [ID](#)^{3a}, R. Turra [ID](#)^{71a}, T. Turtuvshin [ID](#)^{38,aj}, P.M. Tuts [ID](#)⁴¹,
 S. Tzamarias [ID](#)^{152,f}, P. Tzani [ID](#)¹⁰, E. Tzovara [ID](#)¹⁰⁰, F. Ukegawa [ID](#)¹⁵⁷, P.A. Ulloa Poblete [ID](#)^{137c,137b},
 E.N. Umaka [ID](#)²⁹, G. Unal [ID](#)³⁶, M. Unal [ID](#)¹¹, A. Undrus [ID](#)²⁹, G. Unel [ID](#)¹⁶⁰, J. Urban [ID](#)^{28b},
 P. Urquijo [ID](#)¹⁰⁵, P. Urrejola [ID](#)^{137a}, G. Usai [ID](#)⁸, R. Ushioda [ID](#)¹⁵⁴, M. Usman [ID](#)¹⁰⁸, Z. Uysal [ID](#)^{21b},
 V. Vacek [ID](#)¹³², B. Vachon [ID](#)¹⁰⁴, K.O.H. Vadla [ID](#)¹²⁵, T. Vafeiadis [ID](#)³⁶, A. Vaitkus [ID](#)⁹⁶, C. Valderanis [ID](#)¹⁰⁹,
 E. Valdes Santurio [ID](#)^{47a,47b}, M. Valente [ID](#)^{156a}, S. Valentinetti [ID](#)^{23b,23a}, A. Valero [ID](#)¹⁶³,
 E. Valiente Moreno [ID](#)¹⁶³, A. Vallier [ID](#)^{102,an}, J.A. Valls Ferrer [ID](#)¹⁶³, D.R. Van Arneeman [ID](#)¹¹⁴,
 T.R. Van Daalen [ID](#)¹³⁸, A. Van Der Graaf [ID](#)⁴⁹, P. Van Gemmeren [ID](#)⁶, M. Van Rijnbach [ID](#)^{125,36},
 S. Van Stroud [ID](#)⁹⁶, I. Van Vulpen [ID](#)¹¹⁴, M. Vanadia [ID](#)^{76a,76b}, W. Vandelli [ID](#)³⁶, M. Vandenbroucke [ID](#)¹³⁵,
 E.R. Vandewall [ID](#)¹²¹, D. Vannicola [ID](#)¹⁵¹, L. Vannoli [ID](#)^{57b,57a}, R. Vari [ID](#)^{75a}, E.W. Varnes [ID](#)⁷,
 C. Varni [ID](#)^{17b}, T. Varol [ID](#)¹⁴⁸, D. Varouchas [ID](#)⁶⁶, L. Varriale [ID](#)¹⁶³, K.E. Varvell [ID](#)¹⁴⁷, M.E. Vasile [ID](#)^{27b},
 L. Vaslin [ID](#)⁸⁴, G.A. Vasquez [ID](#)¹⁶⁵, A. Vasyukov [ID](#)³⁸, F. Vazeille [ID](#)⁴⁰, T. Vazquez Schroeder [ID](#)³⁶,
 J. Veatch [ID](#)³¹, V. Vecchio [ID](#)¹⁰¹, M.J. Veen [ID](#)¹⁰³, I. Veliscek [ID](#)¹²⁶, L.M. Veloce [ID](#)¹⁵⁵, F. Veloso [ID](#)^{130a,130c},
 S. Veneziano [ID](#)^{75a}, A. Ventura [ID](#)^{70a,70b}, S. Ventura Gonzalez [ID](#)¹³⁵, A. Verbytskyi [ID](#)¹¹⁰,
 M. Verducci [ID](#)^{74a,74b}, C. Vergis [ID](#)²⁴, M. Verissimo De Araujo [ID](#)^{83b}, W. Verkerke [ID](#)¹¹⁴,
 J.C. Vermeulen [ID](#)¹¹⁴, C. Vernieri [ID](#)¹⁴³, M. Vessella [ID](#)¹⁰³, M.C. Vetterli [ID](#)^{142,av}, A. Vgenopoulos [ID](#)^{152,f},
 N. Viaux Maira [ID](#)^{137f}, T. Vickey [ID](#)¹³⁹, O.E. Vickey Boeriu [ID](#)¹³⁹, G.H.A. Viehhauser [ID](#)¹²⁶, L. Vignani [ID](#)^{63b},
 M. Villa [ID](#)^{23b,23a}, M. Villaplana Perez [ID](#)¹⁶³, E.M. Villhauer [ID](#)⁵², E. Vilucchi [ID](#)⁵³, M.G. Vincter [ID](#)³⁴,
 G.S. Virdee [ID](#)²⁰, A. Vishwakarma [ID](#)⁵², A. Visibile [ID](#)¹¹⁴, C. Vittori [ID](#)³⁶, I. Vivarelli [ID](#)¹⁴⁶,
 E. Voevodina [ID](#)¹¹⁰, F. Vogel [ID](#)¹⁰⁹, J.C. Voigt [ID](#)⁵⁰, P. Vokac [ID](#)¹³², Yu. Volkotrub [ID](#)^{86a}, J. Von Ahnen [ID](#)⁴⁸,
 E. Von Toerne [ID](#)²⁴, B. Vormwald [ID](#)³⁶, V. Vorobel [ID](#)¹³³, K. Vorobev [ID](#)³⁷, M. Vos [ID](#)¹⁶³, K. Voss [ID](#)¹⁴¹,
 J.H. Vossebeld [ID](#)⁹², M. Vozak [ID](#)¹¹⁴, L. Vozdecky [ID](#)⁹⁴, N. Vranjes [ID](#)¹⁵, M. Vranjes Milosavljevic [ID](#)¹⁵,
 M. Vreeswijk [ID](#)¹¹⁴, R. Vuillermet [ID](#)³⁶, O. Vujanovic [ID](#)¹⁰⁰, I. Vukotic [ID](#)³⁹, S. Wada [ID](#)¹⁵⁷, C. Wagner [ID](#)¹⁰³,
 J.M. Wagner [ID](#)^{17a}, W. Wagner [ID](#)¹⁷¹, S. Wahdan [ID](#)¹⁷¹, H. Wahlberg [ID](#)⁹⁰, M. Wakida [ID](#)¹¹¹, J. Walder [ID](#)¹³⁴,
 R. Walker [ID](#)¹⁰⁹, W. Walkowiak [ID](#)¹⁴¹, A. Wall [ID](#)¹²⁸, T. Wamorkar [ID](#)⁶, A.Z. Wang [ID](#)¹³⁶, C. Wang [ID](#)¹⁰⁰,
 C. Wang [ID](#)^{62c}, H. Wang [ID](#)^{17a}, J. Wang [ID](#)^{64a}, R.-J. Wang [ID](#)¹⁰⁰, R. Wang [ID](#)⁶¹, R. Wang [ID](#)⁶,
 S.M. Wang [ID](#)¹⁴⁸, S. Wang [ID](#)^{62b}, T. Wang [ID](#)^{62a}, W.T. Wang [ID](#)⁸⁰, W. Wang [ID](#)^{14a}, X. Wang [ID](#)^{14c},

X. Wang ¹⁶², X. Wang ^{62c}, Y. Wang ^{62d}, Y. Wang ^{14c}, Z. Wang ¹⁰⁶, Z. Wang ^{62d,51,62c},
 Z. Wang ¹⁰⁶, A. Warburton ¹⁰⁴, R.J. Ward ²⁰, N. Warrack ⁵⁹, A.T. Watson ²⁰, H. Watson ⁵⁹,
 M.F. Watson ²⁰, E. Watton ^{59,134}, G. Watts ¹³⁸, B.M. Waugh ⁹⁶, C. Weber ²⁹, H.A. Weber ¹⁸,
 M.S. Weber ¹⁹, S.M. Weber ^{63a}, C. Wei ^{62a}, Y. Wei ¹²⁶, A.R. Weidberg ¹²⁶, E.J. Weik ¹¹⁷,
 J. Weingarten ⁴⁹, M. Weirich ¹⁰⁰, C. Weiser ⁵⁴, C.J. Wells ⁴⁸, T. Wenaus ²⁹, B. Wendland ⁴⁹,
 T. Wengler ³⁶, N.S. Wenke ¹¹⁰, N. Wermes ²⁴, M. Wessels ^{63a}, A.M. Wharton ⁹¹, A.S. White ⁶¹,
 A. White ⁸, M.J. White ¹, D. Whiteson ¹⁶⁰, L. Wickremasinghe ¹²⁴, W. Wiedenmann ¹⁷⁰,
 C. Wiel ⁵⁰, M. Wielers ¹³⁴, C. Wiglesworth ⁴², D.J. Wilbern ¹²⁰, H.G. Wilkens ³⁶,
 D.M. Williams ⁴¹, H.H. Williams ¹²⁸, S. Williams ³², S. Willocq ¹⁰³, B.J. Wilson ¹⁰¹,
 P.J. Windischhofer ³⁹, F.I. Winkel ³⁰, F. Winklmeier ¹²³, B.T. Winter ⁵⁴, J.K. Winter ¹⁰¹,
 M. Wittgen ¹⁴³, M. Wobisch ⁹⁷, Z. Wolffs ¹¹⁴, J. Wollrath ¹⁶⁰, M.W. Wolter ⁸⁷, H. Wolters ^{130a,130c},
 A.F. Wongel ⁴⁸, E.L. Woodward ⁴¹, S.D. Worm ⁴⁸, B.K. Wosiek ⁸⁷, K.W. Woźniak ⁸⁷,
 S. Wozniowski ⁵⁵, K. Wraight ⁵⁹, C. Wu ²⁰, J. Wu ^{14a,14e}, M. Wu ^{64a}, M. Wu ¹¹³, S.L. Wu ¹⁷⁰,
 X. Wu ⁵⁶, Y. Wu ^{62a}, Z. Wu ¹³⁵, J. Wuerzinger ^{110,at}, T.R. Wyatt ¹⁰¹, B.M. Wynne ⁵²,
 S. Xella ⁴², L. Xia ^{14c}, M. Xia ^{14b}, J. Xiang ^{64c}, M. Xie ^{62a}, X. Xie ^{62a}, S. Xin ^{14a,14e},
 A. Xiong ¹²³, J. Xiong ^{17a}, D. Xu ^{14a}, H. Xu ^{62a}, L. Xu ^{62a}, R. Xu ¹²⁸, T. Xu ¹⁰⁶, Y. Xu ^{14b},
 Z. Xu ⁵², Z. Xu ^{14c}, B. Yabsley ¹⁴⁷, S. Yacoob ^{33a}, Y. Yamaguchi ¹⁵⁴, E. Yamashita ¹⁵³,
 H. Yamauchi ¹⁵⁷, T. Yamazaki ^{17a}, Y. Yamazaki ⁸⁵, J. Yan ^{62c}, S. Yan ¹²⁶, Z. Yan ²⁵,
 H.J. Yang ^{62c,62d}, H.T. Yang ^{62a}, S. Yang ^{62a}, T. Yang ^{64c}, X. Yang ³⁶, X. Yang ^{14a}, Y. Yang ⁴⁴,
 Y. Yang ^{62a}, Z. Yang ^{62a}, W-M. Yao ^{17a}, Y.C. Yap ⁴⁸, H. Ye ^{14c}, H. Ye ⁵⁵, J. Ye ^{14a}, S. Ye ²⁹,
 X. Ye ^{62a}, Y. Yeh ⁹⁶, I. Yeletsikh ³⁸, B.K. Yeo ^{17b}, M.R. Yexley ⁹⁶, P. Yin ⁴¹, K. Yorita ¹⁶⁸,
 S. Younas ^{27b}, C.J.S. Young ³⁶, C. Young ¹⁴³, C. Yu ^{14a,14e,ax}, Y. Yu ^{62a}, M. Yuan ¹⁰⁶,
 R. Yuan ^{62b}, L. Yue ⁹⁶, M. Zaazoua ^{62a}, B. Zabinski ⁸⁷, E. Zaid ⁵², T. Zakareishvili ^{149b},
 N. Zakharchuk ³⁴, S. Zambito ⁵⁶, J.A. Zamora Saa ^{137d,137b}, J. Zang ¹⁵³, D. Zanzi ⁵⁴,
 O. Zaplatilek ¹³², C. Zeitnitz ¹⁷¹, H. Zeng ^{14a}, J.C. Zeng ¹⁶², D.T. Zenger Jr ²⁶, O. Zenin ³⁷,
 T. Ženiš ^{28a}, S. Zenz ⁹⁴, S. Zerradi ^{35a}, D. Zerwas ⁶⁶, M. Zhai ^{14a,14e}, B. Zhang ^{14c},
 D.F. Zhang ¹³⁹, J. Zhang ^{62b}, J. Zhang ⁶, K. Zhang ^{14a,14e}, L. Zhang ^{14c}, P. Zhang ^{14a,14e},
 R. Zhang ¹⁷⁰, S. Zhang ¹⁰⁶, S. Zhang ⁴⁴, T. Zhang ¹⁵³, X. Zhang ^{62c}, X. Zhang ^{62b},
 Y. Zhang ^{62c,5}, Y. Zhang ⁹⁶, Y. Zhang ^{14c}, Z. Zhang ^{17a}, Z. Zhang ⁶⁶, H. Zhao ¹³⁸, P. Zhao ⁵¹,
 T. Zhao ^{62b}, Y. Zhao ¹³⁶, Z. Zhao ^{62a}, A. Zhemchugov ³⁸, J. Zheng ^{14c}, K. Zheng ¹⁶²,
 X. Zheng ^{62a}, Z. Zheng ¹⁴³, D. Zhong ¹⁶², B. Zhou ¹⁰⁶, H. Zhou ⁷, N. Zhou ^{62c}, Y. Zhou ⁷,
 C.G. Zhu ^{62b}, J. Zhu ¹⁰⁶, Y. Zhu ^{62c}, Y. Zhu ^{62a}, X. Zhuang ^{14a}, K. Zhukov ³⁷, V. Zhulanov ³⁷,
 N.I. Zimine ³⁸, J. Zinsser ^{63b}, M. Ziolkowski ¹⁴¹, L. Živković ¹⁵, A. Zoccoli ^{23b,23a}, K. Zoch ⁶¹,
 T.G. Zorbas ¹³⁹, O. Zormpa ⁴⁶, W. Zou ⁴¹, L. Zwalinski ³⁶.

¹Department of Physics, University of Adelaide, Adelaide; Australia.

²Department of Physics, University of Alberta, Edmonton AB; Canada.

^{3(a)}Department of Physics, Ankara University, Ankara; ^(b)Division of Physics, TOBB University of Economics and Technology, Ankara; Türkiye.

⁴LAPP, Université Savoie Mont Blanc, CNRS/IN2P3, Annecy; France.

⁵APC, Université Paris Cité, CNRS/IN2P3, Paris; France.

⁶High Energy Physics Division, Argonne National Laboratory, Argonne IL; United States of America.

⁷Department of Physics, University of Arizona, Tucson AZ; United States of America.

⁸Department of Physics, University of Texas at Arlington, Arlington TX; United States of America.

⁹Physics Department, National and Kapodistrian University of Athens, Athens; Greece.

¹⁰Physics Department, National Technical University of Athens, Zografou; Greece.

¹¹Department of Physics, University of Texas at Austin, Austin TX; United States of America.

¹²Institute of Physics, Azerbaijan Academy of Sciences, Baku; Azerbaijan.

¹³Institut de Física d'Altes Energies (IFAE), Barcelona Institute of Science and Technology, Barcelona; Spain.

¹⁴(^a)Institute of High Energy Physics, Chinese Academy of Sciences, Beijing; (^b)Physics Department, Tsinghua University, Beijing; (^c)Department of Physics, Nanjing University, Nanjing; (^d)School of Science, Shenzhen Campus of Sun Yat-sen University; (^e)University of Chinese Academy of Science (UCAS), Beijing; China.

¹⁵Institute of Physics, University of Belgrade, Belgrade; Serbia.

¹⁶Department for Physics and Technology, University of Bergen, Bergen; Norway.

¹⁷(^a)Physics Division, Lawrence Berkeley National Laboratory, Berkeley CA; (^b)University of California, Berkeley CA; United States of America.

¹⁸Institut für Physik, Humboldt Universität zu Berlin, Berlin; Germany.

¹⁹Albert Einstein Center for Fundamental Physics and Laboratory for High Energy Physics, University of Bern, Bern; Switzerland.

²⁰School of Physics and Astronomy, University of Birmingham, Birmingham; United Kingdom.

²¹(^a)Department of Physics, Bogazici University, Istanbul; (^b)Department of Physics Engineering, Gaziantep University, Gaziantep; (^c)Department of Physics, Istanbul University, Istanbul; Türkiye.

²²(^a)Facultad de Ciencias y Centro de Investigaciones, Universidad Antonio Nariño, Bogotá; (^b)Departamento de Física, Universidad Nacional de Colombia, Bogotá; (^c)Pontificia Universidad Javeriana, Bogota; Colombia.

²³(^a)Dipartimento di Fisica e Astronomia A. Righi, Università di Bologna, Bologna; (^b)INFN Sezione di Bologna; Italy.

²⁴Physikalisches Institut, Universität Bonn, Bonn; Germany.

²⁵Department of Physics, Boston University, Boston MA; United States of America.

²⁶Department of Physics, Brandeis University, Waltham MA; United States of America.

²⁷(^a)Transilvania University of Brasov, Brasov; (^b)Horia Hulubei National Institute of Physics and Nuclear Engineering, Bucharest; (^c)Department of Physics, Alexandru Ioan Cuza University of Iasi, Iasi; (^d)National Institute for Research and Development of Isotopic and Molecular Technologies, Physics Department, Cluj-Napoca; (^e)University Politehnica Bucharest, Bucharest; (^f)West University in Timisoara, Timisoara; (^g)Faculty of Physics, University of Bucharest, Bucharest; Romania.

²⁸(^a)Faculty of Mathematics, Physics and Informatics, Comenius University, Bratislava; (^b)Department of Subnuclear Physics, Institute of Experimental Physics of the Slovak Academy of Sciences, Kosice; Slovak Republic.

²⁹Physics Department, Brookhaven National Laboratory, Upton NY; United States of America.

³⁰Universidad de Buenos Aires, Facultad de Ciencias Exactas y Naturales, Departamento de Física, y CONICET, Instituto de Física de Buenos Aires (IFIBA), Buenos Aires; Argentina.

³¹California State University, CA; United States of America.

³²Cavendish Laboratory, University of Cambridge, Cambridge; United Kingdom.

³³(^a)Department of Physics, University of Cape Town, Cape Town; (^b)iThemba Labs, Western Cape; (^c)Department of Mechanical Engineering Science, University of Johannesburg, Johannesburg; (^d)National Institute of Physics, University of the Philippines Diliman

(Philippines); (^e)University of South Africa, Department of Physics, Pretoria; (^f)University of Zululand, KwaDlangezwa; (^g)School of Physics, University of the Witwatersrand, Johannesburg; South Africa.

³⁴Department of Physics, Carleton University, Ottawa ON; Canada.

³⁵(^a)Faculté des Sciences Ain Chock, Réseau Universitaire de Physique des Hautes Energies - Université Hassan II, Casablanca; (^b)Faculté des Sciences, Université Ibn-Tofail, Kénitra; (^c)Faculté des Sciences Semlalia, Université Cadi Ayyad, LPHEA-Marrakech; (^d)LPMR, Faculté des Sciences, Université

Mohamed Premier, Oujda;^(e) Faculté des sciences, Université Mohammed V, Rabat;^(f) Institute of Applied Physics, Mohammed VI Polytechnic University, Ben Guerir; Morocco.

³⁶CERN, Geneva; Switzerland.

³⁷Affiliated with an institute covered by a cooperation agreement with CERN.

³⁸Affiliated with an international laboratory covered by a cooperation agreement with CERN.

³⁹Enrico Fermi Institute, University of Chicago, Chicago IL; United States of America.

⁴⁰LPC, Université Clermont Auvergne, CNRS/IN2P3, Clermont-Ferrand; France.

⁴¹Nevis Laboratory, Columbia University, Irvington NY; United States of America.

⁴²Niels Bohr Institute, University of Copenhagen, Copenhagen; Denmark.

⁴³(^a) Dipartimento di Fisica, Università della Calabria, Rende;^(b) INFN Gruppo Collegato di Cosenza, Laboratori Nazionali di Frascati; Italy.

⁴⁴Physics Department, Southern Methodist University, Dallas TX; United States of America.

⁴⁵Physics Department, University of Texas at Dallas, Richardson TX; United States of America.

⁴⁶National Centre for Scientific Research "Demokritos", Agia Paraskevi; Greece.

⁴⁷(^a) Department of Physics, Stockholm University;^(b) Oskar Klein Centre, Stockholm; Sweden.

⁴⁸Deutsches Elektronen-Synchrotron DESY, Hamburg and Zeuthen; Germany.

⁴⁹Fakultät Physik, Technische Universität Dortmund, Dortmund; Germany.

⁵⁰Institut für Kern- und Teilchenphysik, Technische Universität Dresden, Dresden; Germany.

⁵¹Department of Physics, Duke University, Durham NC; United States of America.

⁵²SUPA - School of Physics and Astronomy, University of Edinburgh, Edinburgh; United Kingdom.

⁵³INFN e Laboratori Nazionali di Frascati, Frascati; Italy.

⁵⁴Physikalisches Institut, Albert-Ludwigs-Universität Freiburg, Freiburg; Germany.

⁵⁵II. Physikalisches Institut, Georg-August-Universität Göttingen, Göttingen; Germany.

⁵⁶Département de Physique Nucléaire et Corpusculaire, Université de Genève, Genève; Switzerland.

⁵⁷(^a) Dipartimento di Fisica, Università di Genova, Genova;^(b) INFN Sezione di Genova; Italy.

⁵⁸II. Physikalisches Institut, Justus-Liebig-Universität Giessen, Giessen; Germany.

⁵⁹SUPA - School of Physics and Astronomy, University of Glasgow, Glasgow; United Kingdom.

⁶⁰LPSC, Université Grenoble Alpes, CNRS/IN2P3, Grenoble INP, Grenoble; France.

⁶¹Laboratory for Particle Physics and Cosmology, Harvard University, Cambridge MA; United States of America.

⁶²(^a) Department of Modern Physics and State Key Laboratory of Particle Detection and Electronics, University of Science and Technology of China, Hefei;^(b) Institute of Frontier and Interdisciplinary Science and Key Laboratory of Particle Physics and Particle Irradiation (MOE), Shandong University, Qingdao;^(c) School of Physics and Astronomy, Shanghai Jiao Tong University, Key Laboratory for Particle Astrophysics and Cosmology (MOE), SKLPPC, Shanghai;^(d) Tsung-Dao Lee Institute, Shanghai; China.

⁶³(^a) Kirchhoff-Institut für Physik, Ruprecht-Karls-Universität Heidelberg, Heidelberg;^(b) Physikalisches Institut, Ruprecht-Karls-Universität Heidelberg, Heidelberg; Germany.

⁶⁴(^a) Department of Physics, Chinese University of Hong Kong, Shatin, N.T., Hong Kong;^(b) Department of Physics, University of Hong Kong, Hong Kong;^(c) Department of Physics and Institute for Advanced Study, Hong Kong University of Science and Technology, Clear Water Bay, Kowloon, Hong Kong; China.

⁶⁵Department of Physics, National Tsing Hua University, Hsinchu; Taiwan.

⁶⁶IJCLab, Université Paris-Saclay, CNRS/IN2P3, 91405, Orsay; France.

⁶⁷Centro Nacional de Microelectrónica (IMB-CNM-CSIC), Barcelona; Spain.

⁶⁸Department of Physics, Indiana University, Bloomington IN; United States of America.

⁶⁹(^a) INFN Gruppo Collegato di Udine, Sezione di Trieste, Udine;^(b) ICTP, Trieste;^(c) Dipartimento Politecnico di Ingegneria e Architettura, Università di Udine, Udine; Italy.

⁷⁰(^a) INFN Sezione di Lecce;^(b) Dipartimento di Matematica e Fisica, Università del Salento, Lecce; Italy.

- 71^(a) INFN Sezione di Milano;^(b) Dipartimento di Fisica, Università di Milano, Milano; Italy.
- 72^(a) INFN Sezione di Napoli;^(b) Dipartimento di Fisica, Università di Napoli, Napoli; Italy.
- 73^(a) INFN Sezione di Pavia;^(b) Dipartimento di Fisica, Università di Pavia, Pavia; Italy.
- 74^(a) INFN Sezione di Pisa;^(b) Dipartimento di Fisica E. Fermi, Università di Pisa, Pisa; Italy.
- 75^(a) INFN Sezione di Roma;^(b) Dipartimento di Fisica, Sapienza Università di Roma, Roma; Italy.
- 76^(a) INFN Sezione di Roma Tor Vergata;^(b) Dipartimento di Fisica, Università di Roma Tor Vergata, Roma; Italy.
- 77^(a) INFN Sezione di Roma Tre;^(b) Dipartimento di Matematica e Fisica, Università Roma Tre, Roma; Italy.
- 78^(a) INFN-TIFPA;^(b) Università degli Studi di Trento, Trento; Italy.
- 79 Universität Innsbruck, Department of Astro and Particle Physics, Innsbruck; Austria.
- 80 University of Iowa, Iowa City IA; United States of America.
- 81 Department of Physics and Astronomy, Iowa State University, Ames IA; United States of America.
- 82 Istinye University, Sariyer, Istanbul; Türkiye.
- 83^(a) Departamento de Engenharia Elétrica, Universidade Federal de Juiz de Fora (UFJF), Juiz de Fora;^(b) Universidade Federal do Rio De Janeiro COPPE/EE/IF, Rio de Janeiro;^(c) Instituto de Física, Universidade de São Paulo, São Paulo;^(d) Rio de Janeiro State University, Rio de Janeiro; Brazil.
- 84 KEK, High Energy Accelerator Research Organization, Tsukuba; Japan.
- 85 Graduate School of Science, Kobe University, Kobe; Japan.
- 86^(a) AGH University of Krakow, Faculty of Physics and Applied Computer Science, Krakow;^(b) Marian Smoluchowski Institute of Physics, Jagiellonian University, Krakow; Poland.
- 87 Institute of Nuclear Physics Polish Academy of Sciences, Krakow; Poland.
- 88 Faculty of Science, Kyoto University, Kyoto; Japan.
- 89 Research Center for Advanced Particle Physics and Department of Physics, Kyushu University, Fukuoka ; Japan.
- 90 Instituto de Física La Plata, Universidad Nacional de La Plata and CONICET, La Plata; Argentina.
- 91 Physics Department, Lancaster University, Lancaster; United Kingdom.
- 92 Oliver Lodge Laboratory, University of Liverpool, Liverpool; United Kingdom.
- 93 Department of Experimental Particle Physics, Jožef Stefan Institute and Department of Physics, University of Ljubljana, Ljubljana; Slovenia.
- 94 School of Physics and Astronomy, Queen Mary University of London, London; United Kingdom.
- 95 Department of Physics, Royal Holloway University of London, Egham; United Kingdom.
- 96 Department of Physics and Astronomy, University College London, London; United Kingdom.
- 97 Louisiana Tech University, Ruston LA; United States of America.
- 98 Fysiska institutionen, Lunds universitet, Lund; Sweden.
- 99 Departamento de Física Teórica C-15 and CIAFF, Universidad Autónoma de Madrid, Madrid; Spain.
- 100 Institut für Physik, Universität Mainz, Mainz; Germany.
- 101 School of Physics and Astronomy, University of Manchester, Manchester; United Kingdom.
- 102 CPPM, Aix-Marseille Université, CNRS/IN2P3, Marseille; France.
- 103 Department of Physics, University of Massachusetts, Amherst MA; United States of America.
- 104 Department of Physics, McGill University, Montreal QC; Canada.
- 105 School of Physics, University of Melbourne, Victoria; Australia.
- 106 Department of Physics, University of Michigan, Ann Arbor MI; United States of America.
- 107 Department of Physics and Astronomy, Michigan State University, East Lansing MI; United States of America.
- 108 Group of Particle Physics, University of Montreal, Montreal QC; Canada.
- 109 Fakultät für Physik, Ludwig-Maximilians-Universität München, München; Germany.

- ¹¹⁰Max-Planck-Institut für Physik (Werner-Heisenberg-Institut), München; Germany.
- ¹¹¹Graduate School of Science and Kobayashi-Maskawa Institute, Nagoya University, Nagoya; Japan.
- ¹¹²Department of Physics and Astronomy, University of New Mexico, Albuquerque NM; United States of America.
- ¹¹³Institute for Mathematics, Astrophysics and Particle Physics, Radboud University/Nikhef, Nijmegen; Netherlands.
- ¹¹⁴Nikhef National Institute for Subatomic Physics and University of Amsterdam, Amsterdam; Netherlands.
- ¹¹⁵Department of Physics, Northern Illinois University, DeKalb IL; United States of America.
- ¹¹⁶(^a) New York University Abu Dhabi, Abu Dhabi; (^b) University of Sharjah, Sharjah; United Arab Emirates.
- ¹¹⁷Department of Physics, New York University, New York NY; United States of America.
- ¹¹⁸Ochanomizu University, Otsuka, Bunkyo-ku, Tokyo; Japan.
- ¹¹⁹Ohio State University, Columbus OH; United States of America.
- ¹²⁰Homer L. Dodge Department of Physics and Astronomy, University of Oklahoma, Norman OK; United States of America.
- ¹²¹Department of Physics, Oklahoma State University, Stillwater OK; United States of America.
- ¹²²Palacký University, Joint Laboratory of Optics, Olomouc; Czech Republic.
- ¹²³Institute for Fundamental Science, University of Oregon, Eugene, OR; United States of America.
- ¹²⁴Graduate School of Science, Osaka University, Osaka; Japan.
- ¹²⁵Department of Physics, University of Oslo, Oslo; Norway.
- ¹²⁶Department of Physics, Oxford University, Oxford; United Kingdom.
- ¹²⁷LPNHE, Sorbonne Université, Université Paris Cité, CNRS/IN2P3, Paris; France.
- ¹²⁸Department of Physics, University of Pennsylvania, Philadelphia PA; United States of America.
- ¹²⁹Department of Physics and Astronomy, University of Pittsburgh, Pittsburgh PA; United States of America.
- ¹³⁰(^a) Laboratório de Instrumentação e Física Experimental de Partículas - LIP, Lisboa; (^b) Departamento de Física, Faculdade de Ciências, Universidade de Lisboa, Lisboa; (^c) Departamento de Física, Universidade de Coimbra, Coimbra; (^d) Centro de Física Nuclear da Universidade de Lisboa, Lisboa; (^e) Departamento de Física, Universidade do Minho, Braga; (^f) Departamento de Física Teórica y del Cosmos, Universidad de Granada, Granada (Spain); (^g) Departamento de Física, Instituto Superior Técnico, Universidade de Lisboa, Lisboa; Portugal.
- ¹³¹Institute of Physics of the Czech Academy of Sciences, Prague; Czech Republic.
- ¹³²Czech Technical University in Prague, Prague; Czech Republic.
- ¹³³Charles University, Faculty of Mathematics and Physics, Prague; Czech Republic.
- ¹³⁴Particle Physics Department, Rutherford Appleton Laboratory, Didcot; United Kingdom.
- ¹³⁵IRFU, CEA, Université Paris-Saclay, Gif-sur-Yvette; France.
- ¹³⁶Santa Cruz Institute for Particle Physics, University of California Santa Cruz, Santa Cruz CA; United States of America.
- ¹³⁷(^a) Departamento de Física, Pontificia Universidad Católica de Chile, Santiago; (^b) Millennium Institute for Subatomic physics at high energy frontier (SAPHIR), Santiago; (^c) Instituto de Investigación Multidisciplinario en Ciencia y Tecnología, y Departamento de Física, Universidad de La Serena; (^d) Universidad Andres Bello, Department of Physics, Santiago; (^e) Instituto de Alta Investigación, Universidad de Tarapacá, Arica; (^f) Departamento de Física, Universidad Técnica Federico Santa María, Valparaíso; Chile.
- ¹³⁸Department of Physics, University of Washington, Seattle WA; United States of America.
- ¹³⁹Department of Physics and Astronomy, University of Sheffield, Sheffield; United Kingdom.

- ¹⁴⁰Department of Physics, Shinshu University, Nagano; Japan.
- ¹⁴¹Department Physik, Universität Siegen, Siegen; Germany.
- ¹⁴²Department of Physics, Simon Fraser University, Burnaby BC; Canada.
- ¹⁴³SLAC National Accelerator Laboratory, Stanford CA; United States of America.
- ¹⁴⁴Department of Physics, Royal Institute of Technology, Stockholm; Sweden.
- ¹⁴⁵Departments of Physics and Astronomy, Stony Brook University, Stony Brook NY; United States of America.
- ¹⁴⁶Department of Physics and Astronomy, University of Sussex, Brighton; United Kingdom.
- ¹⁴⁷School of Physics, University of Sydney, Sydney; Australia.
- ¹⁴⁸Institute of Physics, Academia Sinica, Taipei; Taiwan.
- ¹⁴⁹^(a)E. Andronikashvili Institute of Physics, Iv. Javakhishvili Tbilisi State University, Tbilisi;^(b)High Energy Physics Institute, Tbilisi State University, Tbilisi;^(c)University of Georgia, Tbilisi; Georgia.
- ¹⁵⁰Department of Physics, Technion, Israel Institute of Technology, Haifa; Israel.
- ¹⁵¹Raymond and Beverly Sackler School of Physics and Astronomy, Tel Aviv University, Tel Aviv; Israel.
- ¹⁵²Department of Physics, Aristotle University of Thessaloniki, Thessaloniki; Greece.
- ¹⁵³International Center for Elementary Particle Physics and Department of Physics, University of Tokyo, Tokyo; Japan.
- ¹⁵⁴Department of Physics, Tokyo Institute of Technology, Tokyo; Japan.
- ¹⁵⁵Department of Physics, University of Toronto, Toronto ON; Canada.
- ¹⁵⁶^(a)TRIUMF, Vancouver BC;^(b)Department of Physics and Astronomy, York University, Toronto ON; Canada.
- ¹⁵⁷Division of Physics and Tomonaga Center for the History of the Universe, Faculty of Pure and Applied Sciences, University of Tsukuba, Tsukuba; Japan.
- ¹⁵⁸Department of Physics and Astronomy, Tufts University, Medford MA; United States of America.
- ¹⁵⁹United Arab Emirates University, Al Ain; United Arab Emirates.
- ¹⁶⁰Department of Physics and Astronomy, University of California Irvine, Irvine CA; United States of America.
- ¹⁶¹Department of Physics and Astronomy, University of Uppsala, Uppsala; Sweden.
- ¹⁶²Department of Physics, University of Illinois, Urbana IL; United States of America.
- ¹⁶³Instituto de Física Corpuscular (IFIC), Centro Mixto Universidad de Valencia - CSIC, Valencia; Spain.
- ¹⁶⁴Department of Physics, University of British Columbia, Vancouver BC; Canada.
- ¹⁶⁵Department of Physics and Astronomy, University of Victoria, Victoria BC; Canada.
- ¹⁶⁶Fakultät für Physik und Astronomie, Julius-Maximilians-Universität Würzburg, Würzburg; Germany.
- ¹⁶⁷Department of Physics, University of Warwick, Coventry; United Kingdom.
- ¹⁶⁸Waseda University, Tokyo; Japan.
- ¹⁶⁹Department of Particle Physics and Astrophysics, Weizmann Institute of Science, Rehovot; Israel.
- ¹⁷⁰Department of Physics, University of Wisconsin, Madison WI; United States of America.
- ¹⁷¹Fakultät für Mathematik und Naturwissenschaften, Fachgruppe Physik, Bergische Universität Wuppertal, Wuppertal; Germany.
- ¹⁷²Department of Physics, Yale University, New Haven CT; United States of America.
- ^a Also Affiliated with an institute covered by a cooperation agreement with CERN.
- ^b Also at An-Najah National University, Nablus; Palestine.
- ^c Also at APC, Université Paris Cité, CNRS/IN2P3, Paris; France.
- ^d Also at Borough of Manhattan Community College, City University of New York, New York NY; United States of America.
- ^e Also at Center for High Energy Physics, Peking University; China.
- ^f Also at Center for Interdisciplinary Research and Innovation (CIRI-AUTH), Thessaloniki; Greece.

- ^g Also at Centro Studi e Ricerche Enrico Fermi; Italy.
- ^h Also at CERN Tier-0; Switzerland.
- ⁱ Also at CERN, Geneva; Switzerland.
- ^j Also at Département de Physique Nucléaire et Corpusculaire, Université de Genève, Genève; Switzerland.
- ^k Also at Departament de Física de la Universitat Autònoma de Barcelona, Barcelona; Spain.
- ^l Also at Department of Financial and Management Engineering, University of the Aegean, Chios; Greece.
- ^m Also at Department of Physics and Astronomy, University of Sheffield, Sheffield; United Kingdom.
- ⁿ Also at Department of Physics and Astronomy, University of Victoria, Victoria BC; Canada.
- ^o Also at Department of Physics, Ben Gurion University of the Negev, Beer Sheva; Israel.
- ^p Also at Department of Physics, California State University, Sacramento; United States of America.
- ^q Also at Department of Physics, King's College London, London; United Kingdom.
- ^r Also at Department of Physics, Oxford University, Oxford; United Kingdom.
- ^s Also at Department of Physics, Royal Holloway University of London, Egham; United Kingdom.
- ^t Also at Department of Physics, Stanford University, Stanford CA; United States of America.
- ^u Also at Department of Physics, University of Fribourg, Fribourg; Switzerland.
- ^v Also at Department of Physics, University of Massachusetts, Amherst MA; United States of America.
- ^w Also at Department of Physics, University of Thessaly; Greece.
- ^x Also at Department of Physics, Westmont College, Santa Barbara; United States of America.
- ^y Also at Deutsches Elektronen-Synchrotron DESY, Hamburg and Zeuthen; Germany.
- ^z Also at Fakultät Physik , Technische Universität Dortmund, Dortmund; Germany.
- ^{aa} Also at Fakultät für Mathematik und Naturwissenschaften, Fachgruppe Physik, Bergische Universität Wuppertal, Wuppertal; Germany.
- ^{ab} Also at Group of Particle Physics, University of Montreal, Montreal QC; Canada.
- ^{ac} Also at Hellenic Open University, Patras; Greece.
- ^{ad} Also at Institució Catalana de Recerca i Estudis Avançats, ICREA, Barcelona; Spain.
- ^{ae} Also at Institut für Experimentalphysik, Universität Hamburg, Hamburg; Germany.
- ^{af} Also at Institut für Physik, Universität Mainz, Mainz; Germany.
- ^{ag} Also at Institute for Nuclear Research and Nuclear Energy (INRNE) of the Bulgarian Academy of Sciences, Sofia; Bulgaria.
- ^{ah} Also at Institute of Applied Physics, Mohammed VI Polytechnic University, Ben Guerir; Morocco.
- ^{ai} Also at Institute of Particle Physics (IPP); Canada.
- ^{aj} Also at Institute of Physics and Technology, Ulaanbaatar; Mongolia.
- ^{ak} Also at Institute of Physics, Azerbaijan Academy of Sciences, Baku; Azerbaijan.
- ^{al} Also at Institute of Theoretical Physics, Ilia State University, Tbilisi; Georgia.
- ^{am} Also at IRFU, CEA, Université Paris-Saclay, Gif-sur-Yvette; France.
- ^{an} Also at L2IT, Université de Toulouse, CNRS/IN2P3, UPS, Toulouse; France.
- ^{ao} Also at Lawrence Livermore National Laboratory, Livermore; United States of America.
- ^{ap} Also at National Institute of Physics, University of the Philippines Diliman (Philippines); Philippines.
- ^{aq} Also at School of Physics and Astronomy, University of Birmingham, Birmingham; United Kingdom.
- ^{ar} Also at School of Physics and Astronomy, University of Manchester, Manchester; United Kingdom.
- ^{as} Also at SUPA - School of Physics and Astronomy, University of Glasgow, Glasgow; United Kingdom.
- ^{at} Also at Technical University of Munich, Munich; Germany.
- ^{au} Also at The Collaborative Innovation Center of Quantum Matter (CICQM), Beijing; China.
- ^{av} Also at TRIUMF, Vancouver BC; Canada.
- ^{aw} Also at Università di Napoli Parthenope, Napoli; Italy.
- ^{ax} Also at University of Chinese Academy of Sciences (UCAS), Beijing; China.

^{ay} Also at University of Colorado Boulder, Department of Physics, Colorado; United States of America.

^{az} Also at Washington College, Chestertown, MD; United States of America.

^{ba} Also at Yeditepe University, Physics Department, Istanbul; Türkiye.

* Deceased

Journal Pre-proof

Declaration of interests

The authors declare that they have no known competing financial interests or personal relationships that could have appeared to influence the work reported in this paper.

The authors declare the following financial interests/personal relationships which may be considered as potential competing interests:

Journal Pre-proof